DROPLET-BASED MICROFLUIDIC PLATFORMS FOR HIGH-THROUGHPUT DNA GENOTYPING AND AMPLIFICATION

by

Tony J. Zheng

A thesis submitted to Johns Hopkins University in conformity with the requirements for the degree of Masters of Science and Engineering in Biomedical Engineering

Baltimore, Maryland

August 2017

ABSTRACT

Common genetic analysis instruments in genotyping, allele discrimination, and PCR are standardized, indispensable tools in biological, medical, and science research laboratories and R&D industry sectors across the world. Constantly working to improve and create new applications, many fields are looking to construct next-generation technologies that can offer higher throughput, higher efficiency, and lower costs in such genetic analysis techniques. In particular, multinational agricultural companies, in the face of a rapidly growing human population, are working to improve crop production and to accelerate plant breeding and genetic selection techniques in order to maintain global food supplies. These companies, such as DuPont Pioneer we are in collaboration with, are now turning to new microfluidic technologies that present a promising route for miniaturizing and up scaling high-throughput genotyping. Microfluidic technologies reduce sample consumption by thousands, up to millions fold from milliliter volumes to nanoliter droplets, lift processing constraints from discrete 96-well plates to an unlimited, continuous-flow of droplet processing, and downsize of physical footprint from bulky, benchtop instruments to palm-sized, miniaturized devices.

Here, we present two novel microfluidic platforms: 1) a microfluidic platform for multiplexed genotyping of single nucleotide polymorphisms (SNPs), screening a series of DNA targets against a library of probes, achieving 100% accuracy in SNP calling of synthetic maize DNA targets and 93% accuracy in SNP calling of genomic maize DNA targets, using an Invader assay, and 2) a microfluidic platform for integrated, continuous-flow, droplet Taqman-based PCR and end-point allele discrimination. The development of both microfluidic devices offers promising platforms for next generation, high throughput genotyping technologies.

Thesis Readers: Jeff Wang, Ph.D., Dr. Eileen Haase, Ph.D., Dr. Vikram Chib, Ph.D.

ACKNOWLEDGEMENTS

I would like to express my deepest appreciation and gratitude to my thesis advisor and professor, Dr. Jeff Wang and to my tremendous and invaluable mentors, Dr. Wen Hsieh, Dr. Helena Zec, and Dr. Divya Nalayanda, for their continuous teachings, mentorship, patience, and guidance throughout my research projects and experiences. I would also like to thank Anu Kaushik, Dr. Frank Hsieh, and Brant Axt, for their Pioneer research project collaborations, teamwork, and discussions, and the rest of Dr. Wang's lab for their supportive advice, feedback, and insights. Lastly, I would like to thank my family and friends for their constant love and support throughout my Masters program.

TABLE OF CONTENTS

LIST OF FIGURES

CHAPTER 1

CHAPTER 2

CHAPTER 2

CHAPTER 1:

Programmable Microfluidic Genotyping of Plant Samples for Mark-Assisted Selection

---

Note to Reader – this chapter describes a currently submitted manuscript under review for publication:

Zec, H., **Zheng, T.**, Liu, L., Hsieh, K., Rane, T., Pederson, T., Wang, T.H. "Programmable Microfluidic Genotyping of Plant Samples for Marker-Assisted Selection." (2017). In Review.

All experimental design and data were performed and collected by Dr. Helena Zec, Ph.D. and Lily Liu, MSE, thus the following documentation appears in their respective theses. My contributions to the project include: creation of figures and supplementary video, revisions to the written manuscript for resubmission, revision of figures, and replication of experiments for conference proceedings.

1.1 Introduction

In the face of a rapidly growing human population, there is an increasing need to maintain the global food supply [1, 2]. In response, international agricultural companies are now turning to new high-throughput genotyping and DNA marker technologies to improve crop production and accelerate plant breeding [2-4]. In this regard, microfluidic technologies present a promising route for miniaturizing and further scaling up high-throughput genotyping. Unfortunately, traditional microfluidic platforms are limited at processing a large number of unique samples against a flexible panel of markers, which is critical for high-throughput genotyping toward crop development [5-7]. To address this unmet need, we present herein a

highly programmable, microfluidic platform that is capable of genotyping a library of DNA samples against a panel of probes that target various single nucleotide polymorphisms (SNPs). In doing so, our device also overcomes key hurdles in limited sample intake, droplet assembly, and droplet barcoding that have restrained previous droplet-based devices [8]. Specifically, a unique component of our microfluidic platform is the nano sample processor (NSP). Dual NSPs are designed to introduce an unrestricted number of unique DNA samples sequentially into the device via only two inlets, thus overcoming the current limitation to the number of sample inputs due to small device footprint. We implement on the device the Invader assay for SNP genotyping. As an initial demonstration, we achieved 100% accuracy in SNP calling of synthetic maize DNA targets. We then screened eight unique genomic maize DNA targets against 10 SNP-interrogating probes in triplicates in a single droplet-based experiment, and demonstrated 93% accuracy in SNP calling.

1.2 Materials and Methods

1.2.1 Multiplexed PCR

Genomic DNA extracted from eight maize samples were provided by DuPont Pioneer. DNA samples were amplified off-chip using multiplexed PCR prior to the Invader assay [9, 10]. The multiplexed PCR reaction contained 10 primer pairs for simultaneously amplifying 10 loci that contain the 10 target SNPs. Reagents were heated at 95 °C for 600 seconds and then thermocycled for 18 cycles: 95 °C for 30 seconds, 55 °C for 90 seconds, 72 °C for 150 seconds. After thermocycling, a final extension step was executed at 72 °C for 300 seconds. Prior to the SNP Invader assay, amplified genomic DNA targets were denatured at 100 °C for 20 minutes, snap-cooled, and then kept on ice until use for on-chip, droplet-based Invader assay.

1.2.2 Invader Assay and Single Nucleotide Polymorphism Detection

The Invader assay **(Figure 1.1)** is a two-step 63 °C isothermal reaction used to detect single nucleotide polymorphisms (SNPs) for genotyping. The first step of the Invader assay is the recognition of the SNP in the target DNA and the formation of a highly specific tripartite structure. This step consists of four main components: a flap endonuclease (FEN), an Invader oligo, a pair of FAM/RED Invader signal probes, and the target DNA. The Invader oligo contains a complimentary sequence to the 3' end target DNA up to, but not containing the SNP and binds to the target DNA. Similarly, the Invader signal probe has a complimentary sequence to the 5' end target DNA, but contains the complimentary SNP. If the SNP is present on the

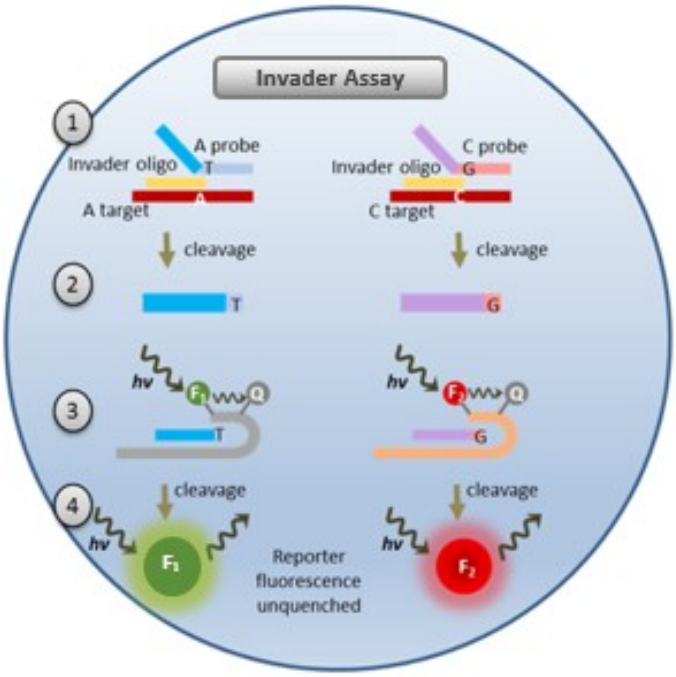

Figure 1.1: The Invader assay consists of the target DNA, Invader oligonucleotide, flap endonuclease (FEN), and a pair of corresponding FAM (green) and RED (red) Invader signal probes and FRET cassettes. **1)** In the primary reaction, both the Invader oligonucleotide and primary probe hybridize to the target of interest. An invasive structure is formed from the single-base overlap. This forms a 3-dimensional structure that is recognized by the FEN cleavase which **2)** cleaves the 5' Arm of the primary probe. **3)** In the secondary reaction, the cleaved 5' arm of the probe binds to the FRET cassette. In this secondary FRET reaction, this structure is recognized by same FEN cleavase which **4)** cleaves the fluorophore and a fluorescent signal is generated.

target DNA, the Invader signal probe binds to the Invader oligo-DNA target, forming a tripartite structure. The FEN cleavase recognizes this specific structure and cleaves the Invader signal probe at the site of the SNP, forming a 5' signal flap. The second step is fluorescence generation. The previously cleaved 5' signal flap binds to a corresponding FAM/RED FRET cassette. The FEN cleavase recognizes this specific structure and cleaves the bounded FAM/RED fluorophore, generating a corresponding FAM/RED signal detected by our optical system. If the SNP was not initially present, the tripartite structure is not formed and the fluorophore remains bounded to the FRET cassette and quenched (no fluorescence is generated). Fluorescence was monitored in FAM (excitation: 450-490 nm and emission: 510-530 nm) and Texas Red (excitation: 560-590 nm and emission: 610-650 nm).

In the assay design stage, 10 polymorphic markers of interest were identified and selected. Each synthetic target set consisted of two oligos, "A" and "B", corresponding to the FAM (green) allele and the RED (red) allele, respectively. For all 10 markers, the Invader probes were designed by Third Wave Technologies. All genomic targets evaluated were known to be homozygous for FAM or RED. All Invader reagents' concentrations are optimized by DuPont Pioneer (Johnston, Iowa) and proprietary.

1.2.3 Device Design

The developed programmable microfluidic Invader device **(Figure 1.2)** consists of two PDMS layers, utilizing a push-up valve architecture, wherein the bottom valve layer **(Figure 1.2, *red*)** collapses into an upper fluidic layer **(Figure 1.2, *green*)**. The fluidic layer features a carrier oil inlet for carrier oil loading, ten probe inlets **(Figure 1.2, P1 – P10)** for Invader probes/reagents, and two unique Nano Sample Processors inlets **(Figure 1.2, S1 and S2)** for DNA sample processing and sample loading/rinsing. The bottom valve layer features corresponding valves aligned underneath each fluidic inlet and channel to automatically control

the opening and closing of each inlet via a custom, programmable MATLAB script. Consequently, DNA samples are digitalized into daughter droplets via the NSPs separated by the immiscible carrier oil and injected with its respective Invader probe in the fusion zone. DNA-probe droplets are then mixed in the serpentine channels, incubated in the incubation zone at 63 ºC for 20 minutes for the Invader reaction, and detected for its fluorescence readout, before exiting via the outlet. All processes occur in a continuous flow manner, akin to an assembly line, allowing for minimal downtime and processing of an unlimited number of

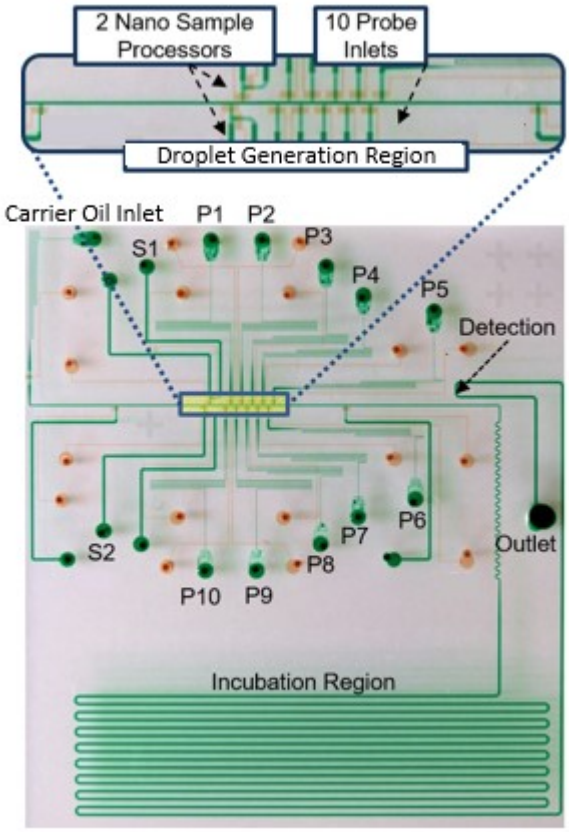

Figure 1.2: Schematic of Invader microfluidic device. The PDMS microfluidic device consists of 2 layers, a bottom valve layer (*red*) and a top fluidic layer (*green*). The fluidic layer features 2 Nano Sample Processors (S1, S2), 10 probe inlets (P1 – P10), and a carrier inlet. Droplets are generated in the droplet generation region and then travel through a serpentine channel which promotes droplet mixing. Once mixed, droplets enter the incubation region and are incubated in continuous flow at 63°C for ~20 minutes. Fluorescence read-out occurs in the detection region, near the outlet of the device using Confocal Fluorescence Spectroscopy.

droplets within the device. With such design, the device can be programmed to analyze multiple, unique DNA samples against a panel of a flexible number of probes. As a proof-of-concept, we screened eight, unique maize DNA samples against a panel of ten Invader probes.

1.2.4 Device Fabrication

Fluidic and valve layer masks were designed in L-EDIT v16.0 (Tanner EDA) and printed by CAD/Art Services, Inc. Fluidic and valve layer molds were fabricated on 4-inch silicon wafers (Polishing Corporation of America). The fluidic layer mold was patterned with SPR 220-7 (MicroChem Corp.) to form the channel regions (height was ~25 μm) to be collapsed by the valve layer. This was followed by patterning of SU8-3025 (MicroChem Corp.) to generate the rest of the fluidic channel network (height was ~45 μm). For the valve layer mold, a single layer of SU8-3025 was patterned on the wafer (height was ~45 μm). The molds were used to fabricate the devices by soft lithography. The fluidic layer molds were first silanized using vapour deposition of chlorotrimethylsilane (Sigma-Aldrich) for 15 minutes. A thick fluidic layer was then casted using 50 grams of PDMS base to crosslinker ratio (6:1) and degassed under vacuum conditions for an hour. The fluidic layer was then cured for eight minutes at 80 °C. The valve layer (15:1, PDMS base to crosslinker ratio) was spun at 1350 RPM (Laurell Technologies, Corp.) and baked for 4 minutes at 80 °C. After baking, the fluidic layer was manually aligned to the valve layer under a stereoscope. Both layers were then baked for 60 minutes at 80 °C. Access holes were then punched for the inlet and outlet ports and the PDMS device was bonded to Thickness #1 cover glass (Ted Pella, Inc.) with oxygen plasma treatment.

1.2.5 Device Priming, Hydrophobic Surface Treatment

The push-up valve architecture of the Invader microfluidic device is compared to the traditional push-down architecture of most microfluidic platforms. In conventional push-down

valve architecture, the fluidic channels reside on a hydrophilic glass surface. The bottom glass surface requires an initial hydrophobic Aquapel (PPG Industries, Pittsburgh, PA) treatment to ensure droplet integrity and stability. Aquapel is filtered using a Syringe Durapore (PVDF) membrane filter unit, 33 mm diameter/0.22 μm pore size (Merck Millipore), and manually injected into the device. Aquapel is flushed out with air at 10 PSI followed by FC40 (3M) at 10 PSI, filtered using a Syringe Nylon membrane filter unit, 30 mm diameter/0.22 μm pore size (CELLTREAT Scientific Products). The device is placed in an oven at 80 ^{o}C for two hours and degassed in a vacuum. In comparison, in push-up valve architecture, Aquapel treatment is not necessary and the Invader microfluidic device is directly degassed in a vacuum prior to use.

1.2.6 Optimization of Carrier Oil, Additives, and Surfactants

Optimization of carrier oil to be used on-chip was performed for the droplet-based Invader assay. Different mixtures of fluorinated oils, including: FC-40, FC-3283, HFE-7500, and 1H, 1H, 2H, 2H-Perfluoro-1-octanol (Sigma Aldrich) (4:1 v/v) (PFO) were evaluated. The addition of bovine serum albumin (BSA) was found to improve small hydrophobic molecule and fluorophore retention within droplets, but caused droplet sticking in the channels and poor droplet mobility. These results were consistent with those found in the literature (11). A mixture of FC-40 and PFO offered the optimal balance between droplet stability and small molecule retention among the carrier oils and surfactants that were evaluated.

1.2.7 Device Operation

A set of solenoid valves was used to control the opening and closing of individual valves in the microfluidic device. The solenoid valves were controlled by a custom MATLAB (Mathworks) program. To interface with the microfluidic device, all reagents were loaded into

Tygon® microbore tubing (Cole-Parmer) and connected with the device through inlet and valve ports. Valves were pressurized at 15 PSI.

The carrier oil, consisting of FC-40 (3M) and 1H, 1H, 2H, 2H-Perfluoro-1-octanol (Sigma Aldrich) (4:1 v/v) (PFO), was pressurized at 5 PSI and loaded into the device via the carrier inlet. The Invader device operation is detailed **(Figure 1.3)**. The carrier oil was allowed to fill and wet the entire length of the central oil channel prior to droplet generation. All reagent/probe inlets were primed and loaded with its respective reagent/probe mixture. Next, the valve actuation sequence was programmed in MATLAB and executed, corresponding to the DNA-probe droplet combinations to be generated in the device. The digitalized DNA droplet (~5 nL) then entered the narrowing fusion zone and thus, stretched to span the entire fusion zone. A mixture containing the respective SNP-interrogating probe, enzymes, and FRET cassettes (~45 nL) was injected in a synchronization-free manner directly into the DNA droplet. Subsequent DNA-probe droplets were continuously processed in an assembly-line manner. Each DNA sample was screened against a library of 10 SNP-interrogating probes, resulting in a sequence containing 10 droplets of different probe composition per DNA sample processed. Following, each DNA-probe droplet passed through a serpentine channel region to promote mixing prior to entering the incubation region. The incubation region was maintained at a constant temperature of 63°C for Invader assay. After incubation, in-line fluorescence readout was performed on droplets using dual laser spectroscopy, where fluorescence intensity data was collected and analyzed.

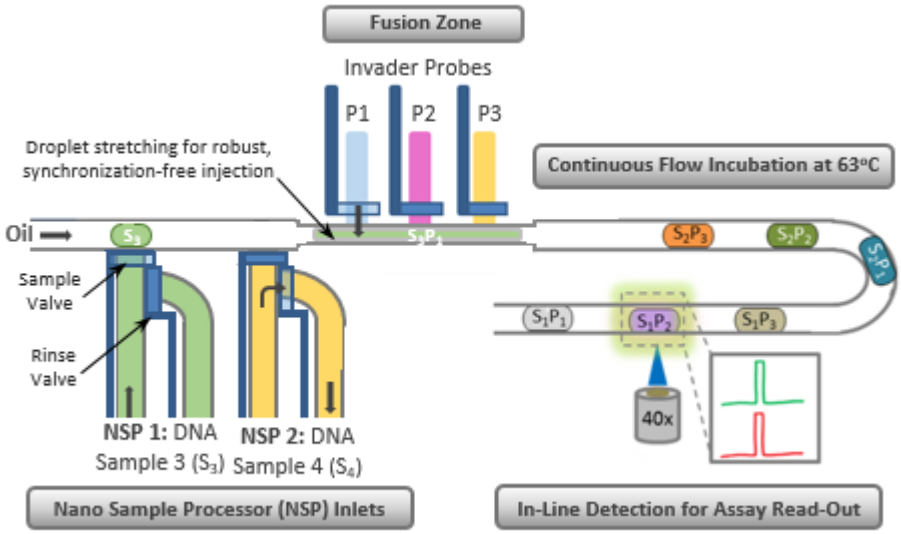

Figure 1.3: DNA samples are sequentially loaded into the microfluidic device via two NSPs and digitalized into ~5 nL droplets. DNA droplets then arrive in the fusion zone, where the narrow channel causes the DNA droplets to stretch and span the entire fusion zone, thus allowing synchronization-free injection of ~45 nL Invader probes and reaction mix into the DNA droplets. DNA-probe droplets are incubated for 20 minutes at 63 ºC as they flow throughout the incubation region in continuous flow. In-line readout is performed and fluorescence signals are then used to determine the final allelic call out for that specific DNA and probe.

1.2.8 Fluorescence Detection and Data Analysis

Spectroscopy data was acquired using a custom-built two-color confocal fluorescence spectroscope (CFS), designed to simultaneously detect both FAM and RED Invader fluorophores within droplets **(Figure 1.4)**. The CFS employs dual laser excitation (488 nm, 552 nm) and dual emission channel (506-534 nm and 608-648 nm), dichroic mirrors, optical band-pass filters, and two silicon avalanche photodiodes (APD) (12). The spectroscopy platform also includes a trans-illumination LED and CCD camera for bright-field imaging (12). Data analysis was performed using custom scripts written in MATLAB (13). The leading and falling edge of each droplet were identified as the location in a fluorescence data trace where

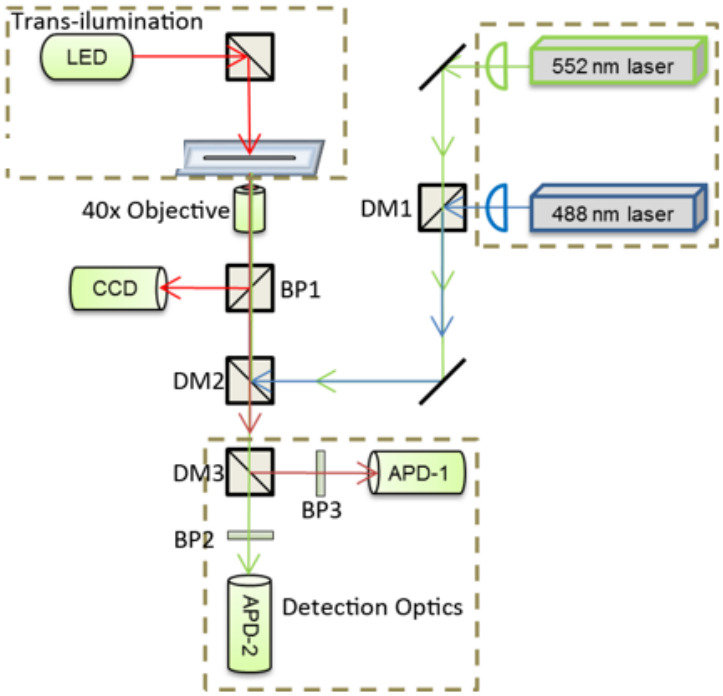

Figure 1.4: The two-color Confocal Fluorescence Spectroscope (CFS) is designed to simultaneously detect fluorescence signals of both Invader probes within droplets. The CFS system employs two laser sources for fluorescence excitation, dichroic mirrors (DM), and optical band-pass filters (BF) for routing optics, and two silicon avalanche photodiodes (APDs) for detection of fluorescence signals. The instrument includes a trans-illumination LED and CCD camera for bright-field imaging of the droplets in the device.

the signal from the FAM fluorescence reached three standard deviations about the background fluorescence of the carrier oil. RED fluorescence data was analyzed at each droplet location, as identified by the FAM signal. Integration time for photon binning was set at 10 *ms* for all peak counting experiments. For each sample, four data traces were analyzed with each trace containing at least 10 visible droplets. MATLAB was used to identify droplets in a data trace and generate the average intensity and standard deviations for each reaction condition across its repeats. The average droplet intensity of each droplet was then used to determine the final allelic call out for that specific DNA-probe combination. The average fluorescence intensity of

a DNA-probe combination droplet was divided by the average fluorescence intensity of a probe-only control droplet. Data was analyzed according to the following calculation (14):

$$\text{Equation 1: } \log\left(\frac{FAM}{RED}ratio\right) = \log\left(\frac{\frac{RFU_{FAM_{sample}}}{RFU_{FAM_{average_{no_{target_{control}}}}}}}{\frac{RFU_{RED_{sample}}}{RFU_{RED_{average_{no_{target_{control}}}}}}}\right)$$

1.3 Results and Discussion

1.3.1 Sample Loading via Nano Sample Processors

We present a programmable, droplet-based microfluidic platform that is capable of multiplexed SNP genotyping a library of maize DNA samples against a panel of SNP markers. The device features a unique, high-throughput dual Nano Sample Processor (NSP) technology, robust synchronization-free probe injection, and in-line continuous incubation and detection for assay read-out **(Figure 1.3)**. Dual NSPs are designed to optimally load multiple samples sequentially into the device **(Figure 1.5)**. In operation, two NSPs (NSP 1 and NSP 2) are functionalized in unison **(Figure 1.5A)**. As NSP 1 digitalizes DNA Sample 1 into daughter droplets into the central oil channel of the device, the upcoming DNA Sample 2 is pressurized and loaded into NSP 2 **(Figure 1.5A, Step 1)**. Upon completed droplet generation by NSP 1, the function of each NSP switches. NSP 2 now digitalizes DNA Sample 2 into daughter droplets, while NSP 1 rinses the previous DNA Sample 1 out of the device and loads the upcoming DNA Sample 3 **(Figure 1.5A, Step 2)**. Continuously, the process repeats, NSP 1 returns to droplet generation and digitalizes DNA Sample 3 into daughter droplets, as NSP 2 now undergoes rinsing and is ready to load new, subsequent samples **(Figure 1.5A, Step 3)**. As such, when dual NSPs are functionalized in unison, a continuous workflow of sample loading, droplet generation, and rinsing is achieved without stopping the flow of the droplets in processing regions downstream in the device, thus minimizing the downtime. This dual NSP technology allows for clean and efficient loading and processing of a high number of unique

DNA samples via only two sample inlets, bypassing current limitations of restricted device size and footprint that can only house 10 to 30 inlets. Finally, this design is even more advantageous when the dual NSP technology is interfaced with a robotic multi-well sampling system (15), allowing the presented system to be operated in an automatic manner for high throughput sampling applications.

A single NSP functions for robust and rapid sample loading, droplet generation, and sample rinsing **(Figure 1.5B)**. The working mechanism for loading multiple samples is visually demonstrated using green and yellow dye in a step-by-step manner. First, the sample valve is closed and the rinse valve is opened as green dye is pressurized and rapidly loaded into the NSP via the sample inlet **(Figure 1.5B, Step 1)**. After loading is completed, the rinsing valve is closed. The sample valve is now actuated, digitalizing the green dye into daughter droplets into the central oil channel **(Figure 1.5B, Step 2)**. Daughter droplets' size can be precisely controlled by programmable actuation of the sample valve, precisely tuning the duration of opening and closing of the valve. Following droplet generation, the sample valve is closed and the rinse valve is opened in which rinsing fluid followed by compressed air is flown through the NSP to clean and drive residual green dye out of the NSP **(Figure 1.5B, Step 3)**. After the NSP is sufficiently rinsed, a new yellow dye is loaded into the NSP and following, the rinsing valve is closed **(Figure 1.5B, Step 4)**. The sample valve is again actuated and yellow dye is digitalized into daughter droplets into the central oil channel **(Figure 1.5B, Step 5)**. In operation, two NSPs are functionalized in unison, with each NSP alternating between sample droplet generation and sample loading/rinsing. This dual NSP technology allows for a continuous workflow of droplet generation with minimal downtime, more efficient throughput.

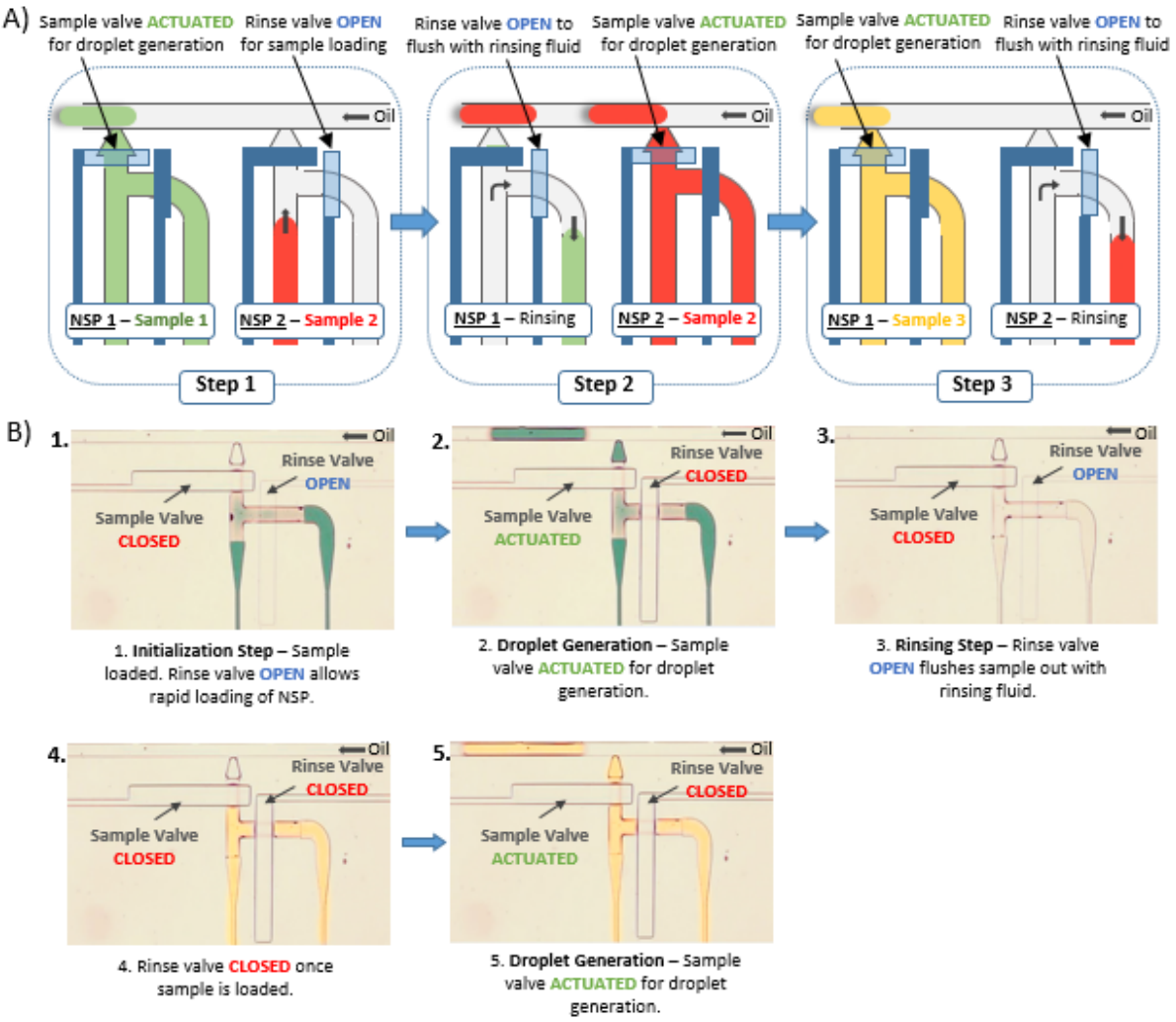

Figure 1.5: A) In the microfluidic platform, switchable dual Nano Sample Processor inlets (NSP 1 and NSP 2) are used in tandem to process potentially unrestricted number of unique samples while minimizing downtime. **Step 1)** DNA Sample 1 is pressurized and loaded into NSP 1. As NSP 1 digitalizes DNA Sample 1 into a series of ~5 nL daughter droplets into the central oil channel, DNA. Sample 2 is loaded into NSP 2. **Step 2)** Once NSP 1 finishes digitalizing droplets from DNA Sample 1, the function of each NSP switches. NSP 2 immediately follows and digitalizes DNA Sample 2 into daughter droplets, while NSP 1 undergoes the rinsing step, during which the rinsing valve opens and allows rinsing fluid followed by compressed air to flush and clear residual Sample 1 from the NSP. Sample 3 is then loaded into NSP 1. **Step 3)** The function of each NSP switches back: NSP 1 digitalizes DNA Sample 3 into daughter droplets. Simultaneously, NSP 2 undergoes rinsing and loads the subsequent DNA sample. This switchable, dual NSP technology enables continuous and alternating sample processing and sample rinsing of potentially an unrestricted number of unique samples into the device via only two sample inlets with minimal idle time

Figure 1.5 (Cont.) B) Step-by-step operation of NSP in processing consecutive, unique samples is visually demonstrated with green and yellow food dyes.**1) Initialization Step.** By closing the sample valve and opening the rinse valve, green dye is rapidly loaded into the NSP, without flowing into the central oil channel. Once the green dye has been loaded, the rinsing valve is closed. **2) Droplet Generation Step.** The sample valve is actuated for droplet generation, digitalizing green dye into daughter droplets into the central oil channel. **3) Rinsing Step.** Following droplet generation, the sample valve is closed and the rinsing valve is opened. Rinsing fluid and compressed air is flown through the NSP to clean and drive the unused green dye out of the NSP. **4) Initialization Step.** Following rinsing, yellow dye is loaded into the NSP and the rinsing valve is closed. **5) Drop Generation Step.** The sample valve is again actuated and yellow dye is digitalized into daughter droplets.

1.3.2 Benchtop Verification of Invader Assay

The Invader assay is successfully verified for single-stranded synthetic DNA samples on benchtop experiments. The results of the bench-top reactions served as a reference for device performance of droplet reactions and empirically establish reliable metrics for data analysis. In this work, we used five pairs of synthetic maize DNA samples (directly provided and denoted by DuPont Pioneer as sample 4, 5, 6, 7, and 9) that target 5 distinct SNP markers and are detected via their respective Invader probe sets. Each pair of DNA samples differs by only a single nucleotide (labelled either as "A" for the RED allele or as "B" for the FAM allele). Here, reaction mixtures containing the reaction buffer, $MgCl_2$, Invader probes, Cleavase, FRET cassettes, and synthetic targets were incubated at 63 °C in a real-time PCR machine while FAM (green) and Redmond Red (red) fluorescence signals from these reactions were measured throughout the reaction. For all five pairs of synthetic targets and corresponding Invader probe sets, fluorescence intensities increased exponentially immediately after the reactions commenced and plateaued after approximately 6 minutes, indicating that the cleavage of the fluorophores from all FRET cassettes had been exhausted **(Figure 1.6A)**. The time necessary to reach steady-state fluorescence levels was incorporated into the microfluidic chip design,

and determined the minimum incubation channel length. Moreover, the allele detection was specific as expected, as targets "A" in all five pairs of targets resulted in an increase in only RED fluorescence and targets "B" in all five pairs of targets resulted in an increase in only FAM fluorescence **(Figure 1.6B)**.

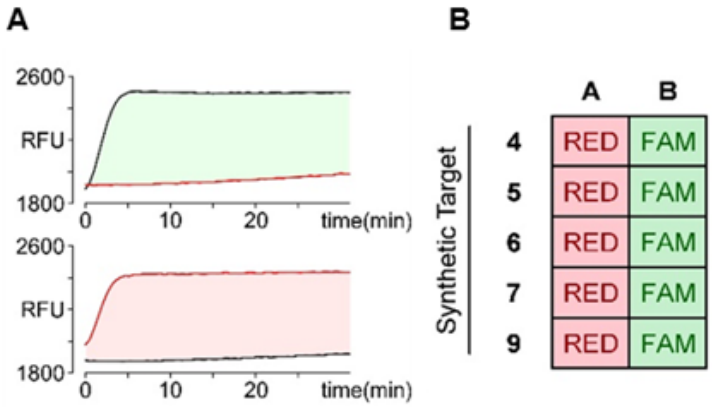

Figure 1.6: Bench-top SNP Genotyping Invader Assay Results. **A)** Representative curves observed from the CFX96 real-time machine. The Invader reaction was incubated at 63°C and a fluorescence reading was taken every 30 seconds. Within less than 10 minutes the Invader reaction reached a plateau. Allele call-outs were performed by taking the ratio of the end-point intensities of the FAM to RED fluorescence. If the log of FAM/RED ratio was < -0.39, the call was determined to be RED. If the ratio was > -0.07, the call was FAM. If the ratio was equal or in between the values, the call was determined be positive for both FAM and RED. These values were empirically determined as the threshold value using synthetic heterozygous DNA samples. In this example, the top graph would yield a FAM call and the bottom would yield a RED call. **B)** Bench top Invader read out of synthetic target pairs with their corresponding probes. FAM represents the allele corresponding to the probe containing the FAM fluorophore ("B" target), and vice versa for RED as Redmond Red ("A" target). Allele call outs were correct for 100% of the cases.

1.3.3 Fluorescence Detection of Invader Products in Droplets

Successful on-chip Invader assay in the droplet format is predicated on robust fluorescence detection of Invader reaction products within droplets. As such, we digitized Invader reaction products that were first completed on benchtop into droplets and used our two-color confocal

fluorescence spectroscopy system to detect the fluorescence within the droplets. Based on the detected fluorescence, we first optimized the carrier oil composition that best retained fluorescence molecules within the droplet from droplet generation to detection. A mixture of FC-40 and 1H, 1H, 2H, 2H-Perfluoro-1-octanol (PFO) (4:1 v/v) offered the optimal balance between droplet stability and small molecule retention among carrier oils and surfactants that were evaluated.

We also found that hydrophobic treatment of the device's fluidic channel surfaces was detrimental to fluorescence detection and we therefore modified our device architecture to obviate such surface treatment. Conventionally, droplet-based, microfluidic devices employ a push-down valve architecture, wherein the fluidic layer is located below the valve layer **(Figure 1.7A, top).** In such configuration, droplets flow directly over the bottom glass surface. Due to the glass's hydrophilicity, it needs to be treated with Aquapel to render the surface hydrophobic, allowing droplets to flow smoothly through the device (16, 17). However, Aquapel treatment is observed to be incompatible with the Invader assay, causing adsorption of small hydrophobic molecules, including FAM and Redmond RED fluorophores, out of the droplets and onto the PDMS channel walls. These effects further exacerbated at 63 ºC, such that the end-point fluorescence signals significantly decreased over time and was indistinguishable from the carrier oil phase **(Figure 1.7A, bottom)**. To solve this problem, a push-up valve architecture was adopted, wherein the fluidic layer is located above valve layer **(Figure 1.7B, top)**. In this new design, droplets travel on the innately hydrophobic PDMS surface, which obviates hydrophobic surface treatment. End-point fluorescence signals were not only significantly

higher than those observed with a push-down architecture, but also maintained stable signals at elevated temperatures over time **(Figure 1.7B, bottom)**.

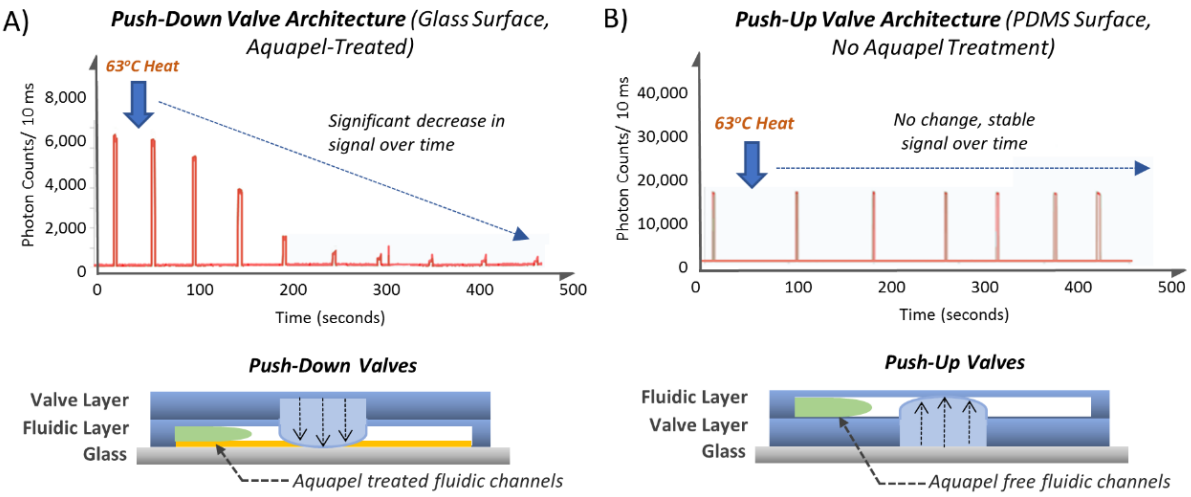

Figure 1.7: A) In the push-down valve architecture, wherein the fluidic layer is located below the valve layer, droplets come into direct contact with the bottom glass surface **(Figure 1.7A, top)**. This architecture requires an initial Aquapel treatment of the bottom glass surface to ensure stable droplet mobility and integrity. Unfortunately, such Aquapel-treated device causes detrimental loss in fluorescence signals of Invader reaction products that are digitalized into droplets at 63 °C **(Figure 1.7A, bottom)**. B) In contrast, push-up valve architecture, wherein the fluidic layer is located above the valve layer, droplets are surrounded by PDMS **(Figure 1.7B, top)** and can maintain stable mobility and integrity even without Aquapel treatment. By obviating Aquapel treatment, the fluorescence signals of Invader reaction products display significantly higher intensities and remain stable at 63 °C over time **(Figure 1.7B, bottom)**.

1.3.4 On-Chip Genotyping of Synthetic DNA Samples

On-chip, droplet-based Invader assay of five sets of synthetic maize DNA samples (directly provided and denoted by DuPont Pioneer as sample 4, 5, 6, 7, and 9) achieved 100% correct callout. In this experiment, each of the five synthetic DNA targets is paired with an allele probe "A" and "B," denoting Redmond Red (red) and FAM (green), respectively. Each sample is loaded sequentially into the device, where sample "A" is loaded through one NSP and sample

"B" is loaded through the other NSP. Each sample is digitalized into droplets in an asymmetrical sequence of *B, B, A* and injected with its corresponding allele probe in the fusion zone. This asymmetric arrangement would ensure that the resulting droplets' identities could be readily determined from the fluorescence data based on which synthetic DNA sample was generated as a duplicate. After injection of corresponding Invader probes and the reaction mixture and incubation at 63 °C for ~20 minutes, the fluorescence within droplets was measured as the droplets flowed through the detection region. The height of the droplets is directly correlated with the droplet fluorescence intensity. Moreover, multiple sequences of synthetic DNA droplets were collected, demonstrating that the sequence of droplets is maintained as they move from the droplet generation to droplet detection **(Figure 1.8A)**.

The average fluorescence intensities are determined for each synthetic target set **(Figure 1.8B)**. The fluorescence intensities for each combination of DNA sample and Invader probe only vary slightly, which is evident by the small error bars. However, the fluorescence intensities differ significantly across DNA sample sets. For example, synthetic target pairs 6 and 7 are high in amplitude and 9 is very low. Thus, the fluorescence intensity alone cannot be used to reliably call the alleles. To this end, a ratiometric analysis is used to accurately determine allele calling. The numeric value for the FAM/RED ratios is shown for each individual synthetic target set in **Figure 1.8B** as well.

The log ratios of FAM/RED fluorescence intensities for each synthetic target sets 4, 5, 6, 7, and 9 paired with Redmond RED allele "A" (red) and FAM allele "B" (green) are calculated and used to determine the SNP allele present in each synthetic target/allele pair, achieving a 100% SNP call out in all 15 reactions **(Figure 1.8C)**. The final allele call-out guidelines were then determined based on this empirically measured ratio. A ratio of greater than -0.07 would result in a FAM call, while a ratio smaller than -0.39 would result in a RED call. A ratio equal

to or between [-0.39: -0.07] resulted in a positive call for both FAM and RED (equivalent to a heterozygous call). As expected for each synthetic target pair, all “A” targets (homozygous) yielded a RED (red) call, and all “B” targets (homozygous) yielded a FAM (green) call. All “AB” targets (heterozygous), yielded a positive FAM and RED call. A comparison with the bench top data show that the on-chip Invader assay with synthetic target achieved a 100% correct call out for each synthetic allele. The thresholds for allele calling that were empirically determined using synthetic targets were used as metrics for data analysis of genomic targets.

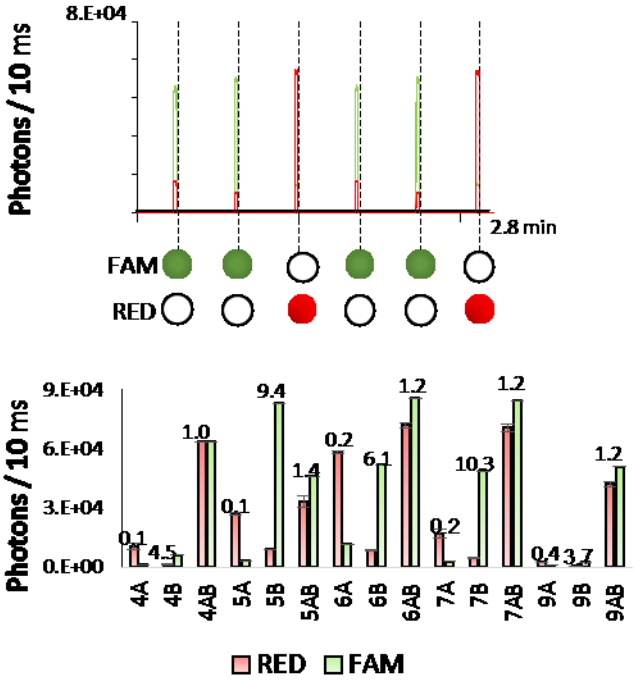

Allele Type

Synthetic DNA	A	B	AB	
4	-1.31	0.27	-0.39	*
5	-1.33	0.58	-0.07	**
6	-1.09	0.28	-0.23	
7	-1.10	0.61	-0.14	
9	-0.82	0.24	-0.33	

Figure 1.8: A) Representative trace of synthetic target 6 FAM and RED fluorescence from on-chip, real-time read out of the Invader assay consists of two repeats of the same asymmetrical sequence, *B, B, A*. The first two peaks correspond to droplets containing synthetic target B and the third corresponds to droplets containing synthetic target A. B) The average fluorescence intensities of synthetic target sets 4, 5, 6, 7 and 9 are calculated. For each synthetic target/marker, the fluorescence intensities differed in magnitude. As a result, the ratio of FAM/RED intensity was used for allele calling. Please note that the data shown here is prior to normalization to NTC droplets. C) The log ratios of FAM/RED intensities of each synthetic target sets 4, 5, 6, 7, and 9 paired with allele "A" and allele "B" were calculated. As expected, all "B" targets yielded a FAM call, and all "A" targets yielded a RED call. All "AB" targets (heterozygous), yielded a positive FAM and RED call. Allele-calling cut off values were empirically determined from the minimum and maximum ratios of the heterozygous target (*Synthetic Target 4 and **Synthetic Target 5). Data has been normalized to NTC droplets (as shown in Equation 1).

1.3.5 On-Chip Genotyping of Genomic Invader DNA Targets

On-chip multiplexed SNP genotyping of eight genomic maize DNA samples (directly provided and denoted by DuPont Pioneer as sample 1-8) against 10 Invader probe sets was successfully performed with 93% accuracy of call out for each allele **(Figure 1.9)**. Multiplexing was performed as described above and sequences of 10 droplets (one DNA sample at a time with each of the 10 probes) were generated continuously. Of the total 80 combinations, five resulted in an ambiguous call when compared to the bench top results (6.3%). However, each of these ambiguous call outs exhibits a log(FAM/RED) ratio in the heterozygous range, suggesting that additional data points for these particular cases may be necessary or that the assay design requires further optimization. Furthermore, the standard deviations calculated for n=3 per DNA/probe combination had low variation suggesting that the signals observed and consequent allelic call outs were robust. On-chip collected genotypic fingerprints for all eight maize samples matched the bench-top reactions.

Of note, accurate SNP calling from successive DNA samples indicate that cross-contamination between DNA samples was negligible in the device even when DNA samples were sequentially processed through the dual NSP inlets. Specifically, because each DNA sample had different SNP patterns for each marker studied, they were ideal samples to ensure the lack of cross-contamination. It is important to note that the Invader assay can perform up to a million-fold amplification, thus had there been any cross-contamination between successive samples, this would have likely been observed during detection. Therefore, the rinse channel of the NSP was found to be highly effective in curtailing cross-contamination between successive genomic DNA samples, and would likely to be able to be employed in platforms that utilize other amplification-based assays, i.e. the Polymerase Chain Reaction.

Genomic DNA \ Probe	1	2	3	4	5	6	7	8	9	10
1	0.74	0.07	0.16	0.13	0.03	0.02	0.00	0.02	0.04	0.05
2	0.76	0.69	-1.29	0.63	-0.24	-1.58	0.89	-1.18	-1.29	-0.96
3	-0.31	-1.06	-1.26	-1.46	-0.98	0.63	0.89	-1.17	-1.17	-0.23
4	0.70	0.68	-0.01	-1.47	-1.47	-1.43	0.89	-0.96	-0.96	-0.64
5	0.71	0.67	-1.06	-1.52	0.84	-1.33	-0.75	-1.11	-1.20	-0.71
6	0.72	0.67	0.00	-1.60	0.89	0.73	0.78	-0.20	-1.09	-0.63
7	-0.35	-0.42	0.18	-1.64	-0.96	0.72	0.87	-0.54	-1.26	-0.86
8	0.69	0.63	-0.94	-1.58	-1.37	0.73	0.88	-1.02	-0.03	-0.77

RED	< -0.39
Heterozygous	[-0.39 : -0.07]
FAM	> -0.07

Figure 1.9: Call-out table, the log of the average ratio of FAM/RED fluorescence intensities for all 80 multiplexed reactions with 8 genomic Maize DNA targets against 10 Invader SNP marker probes, is calculated and plotted here. Droplet sequences of 10 probes in sequential order were used for all genomic targets. Allele type is displayed in the chart as either green (FAM allele) or red (Redmond Red allele), with a log ratio less than -0.39 and ratio greater than -0.07, respectively. Of 80 averaged reactions, only 5 resulted in a mismatched call (DNA 2 with probe 5, DNA 3 with probes 1 and 10, DNA 6 with probe 8, DNA 7 with probes 1), resulting in a 93.8% call accuracy.

1.4 Conclusion

This microfluidic platform represents the first embodiment of a droplet-based, continuous flow platform for agricultural applications. The presented Nano Sample Processor rectifies limitations to the number of unique samples that can be introduced on to the microfluidic device because of small footprint. By employing a valve-based reagent/probe fusion scheme, the microfluidic device was able to perform combinatorial screening, where most microfluidic platforms cannot. The ability to alternate sample droplet generation between two different NSPs significantly eliminates downtime, while maintaining sample rinsing/loading and droplet processing downstream. In future iterations of the device, the dual NSP design can be integrated with probe inlets, allowing probes and samples to be switched on-demand and enhancing flexibility in setting up screening reactions. When coupling the device to a robotic sampling

system (15), the presented system can be operated in an automatic manner for high throughput applications. Furthermore, the cost per screening assay is dramatically lessened by reducing the reaction volume from 5 μL down to 50 nL. We believe the device presented herein has the potential to fulfil the unmet need for increased miniaturization, flexibility and scalability in genomic selection for cultivar development.

CHAPTER 2:

Continuous-Flow, Droplet-Based Microfluidic PCR Platform for DNA Amplification

2.1 Introduction

As detailed in the previous chapter, the Invader microfluidic device requires an initial preparation PCR step, in which the SNP containing DNA sequence is amplified in a separate, off-chip module prior to device operation. This step was crucial in such that only the SNP sequences specific to the probes were amplified and a sufficient amount was created for the Invader assay to take place. Conversely, on-chip, continuous-flow PCR was not achievable due to the high temperature requirement of 95 ^{o}C needed for thermocycling, leading to issues in evaporation, small molecule and fluorophore diffusion, and poor temperature control and temperature variations in the heating system. In this chapter, we describe the development of a fully integrative microfluidic platform capable of performing both on-chip, continuous-flow, droplet-based PCR and end-point allele discrimination/genotyping, using a Taqman-based PCR assay.

2.2 Materials and Methods

2.2.1 Taqman-Based PCR Assay

The Taqman-based PCR assay combines PCR amplification with Taqman probe polymerization of the corresponding DNA target of interest to detect single nucelotide polymorphisms (SNPs). The Taqman-based PCR assay reagents consist of the DNA sequence of interest, corresponding DNA primers and Taqman probes, and an optimized KlearKall Master mix, containing Taqman polymerase, optimized buffer solution, dNTPs, and a ROX

reference dye. The Taqman PCR assay utilizes an initial three-minute 95 ºC hot start to activate the Taqman polymerase enzyme followed by a two-temperature thermocycling for DNA denaturation at 92 ºC for 45 seconds and DNA amplification and annealing at 60 ºC for 45 seconds. This is thermocycled for 30 cycles.

Each set of Taqman probes consists of the same sequence, differing only at the location of the SNP. A FAM/VIC fluorophore corresponding to the two SNPs is attached to one end of the Taqman probe and a quencher is attached to the other end. The close proximation of quencher to the fluorophore on the probe inhibits the fluorophore's fluorescence. In the first step of thermocycling at 92 ºC, the DNA template is denatured into single stranded DNA. In the second step of thermocycling at 60 ºC, the DNA primer binds to the single stranded DNA template and the specific SNP-containing Taqman probe hybridizes to the complementary sequence on the DNA template. DNA polymerase adds the complementary dNTPs to the DNA template, amplifying the product. As the DNA polymerase reaches the hybridized Taqman probe, it cleaves the bound fluorophore from the Taqman probe, releases it from the quencher, and generates a corresponding FAM/VIC fluorescence detected by our optical setup. If the DNA template does not contain the complementary SNP to the Taqman probe, the Taqman probe does not hybridize to the DNA sequence, and the fluorophore remains bound to the probe and quenched. Thus, the detected fluorescence signal serves as a both an indication of successful, specific DNA amplification and SNP detection/genotyping.

All reagents are supplied and optimized by DuPont Pioneer and proprietary. Several target DNA used in development, targets with homozygous alleles for FAM fluorescence, homozygous alleles for VIC fluorescence, and heterozygous alleles for FAM/VIC fluorescence. For each experiment on-chip, a 50 uL is prepared, consisting of 25 uL of KlearKall buffer, 5 uL of target DNA template, and 5 uL of corresponding probe. A negative control is used in

which the DNA template of interest is substituted with water. Lastly, a 50 uL aliquot of ROX reference dye is used as a spatial indicator.

2.2.2 Device Design

The developed microfluidic PCR device (**Figure 2.1**) designed for the Taqman-based assay consists of two PDMS layers, utilizing a push-up valve architecture, wherein the bottom PDMS valve layer (**Figure 2.1, *red***) valves pushes up and collapses into an upper PDMS fluidic layer (**Figure 2.1, *green***). Architecture-wise, the microfluidic PCR device is designed as a simplified and modified Invader device. The fluidic layer features an oil inlet for carrier oil loading, five sample/reagent inlets for sample/reagent loading and droplet generation in the assembly zone, followed by a heating region. The heating region consists of a long channel for the initial, hot-start step of PCR and serpentine channels of 30 turns for the 30 cycles of thermocycling. The device is interfaced to a heating plate such that the long channel and half of the serpentine channels are on a 92 ºC Peltier plate and the other half of the serpentine channels are on a 60 ºC Peltier plate. The specific lengths and turns of the channel geometry is

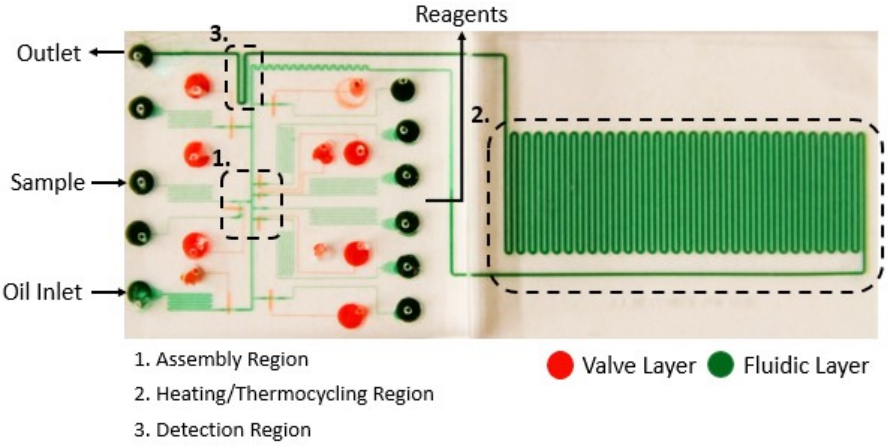

Figure 2.1: Schematic of microfluidic PCR device. Fluidic layer (green) features an oil inlet for loading of carrier oil, five sample/reagent for sample/reagent loading and droplet generation in the assembly region, serpentine channels in the heating region for thermocycling, and a detection region for fluorescence detection and measurement. The valve layer (red) features corresponding valves directly underneath each fluidic channel sample/oil inlet that controls the opening and closing of each.

optimized to meet the required PCR timing conditions needed for each temperature zone. After thermocycling, droplets travel through a detection region where FAM/VIC fluorescence is measured before exiting via the outlet.

The Taqman-based PCR mixture is prepared on benchtop. Each sample is loaded into Tygon® tubing and interfaced loaded into the device via the sample inlets. The sample is then digitalized into daughter droplets via a custom MATLAB script that automates the actuation of the corresponding sample channel valve to generate droplets. The DNA droplets are separated by and travel in an immiscible carrier oil. The microfluidic device is secured onto a custom heating and optical detection platform and thermocycled in the heating region. The speed of the droplets is optimized by the back-pressure flow of the carrier oil to achieve sufficient thermocycling time for the Taqman-based PCR to occur in each temperature zone. After complete thermocycling, the droplets exit the heating region and the FAM/VIC fluorescence is measured in the detection region, before exiting via the outlet. All processes occur in continuous flow, allowing for minimal downtime and continuous sample droplet generation, thermocycling, and detection of an unlimited number of droplets, akin to an assembly belt.

2.2.3 Device Fabrication

Fluidic and valve layer masks were designed in L-EDIT v16.0 (Tanner EDA) and printed by CAD/Art Services, Inc. Fluidic and valve layer molds were fabricated on 4-inch silicon wafers (Polishing Corporation of America). The fluidic layer mold was patterned with SPR 220-7 (MicroChem Corp.) to form the channel regions ~25 μm in height to be collapsed by the valve layer, ~100 μm in height in the droplet generation channel region, and stepped up to ~200 μm in height for the heating channel region and outlet channel. The increase in channel

height decreases the droplets' surface area to volume ratio, minimizing the amount of contact of the droplets with the PDMS channel walls and thus, decreasing the degree of evaporation. For the valve layer mold, a single layer of SU8-3025 (MicroChem Corp.) was patterned on the wafer (height was ~45 μm).

The molds were used as a template to fabricate the devices by soft lithography using PDMS from SYLGARD 184 (Ellsworth). Two types of devices were fabricated: an initial "thick" chip similar to the Invader device fabrication process and later, an improved "thin" chip to mitigate evaporation issues. The fluidic layer mold was first silanized using vapour deposition of chlorotrimethylsilane (Sigma-Aldrich) for 5 minutes. In the thick chip preparation, the fluidic layer was then casted using 50 grams of PDMS base to crosslinker ratio (6:1) and degassed under vacuum conditions for 30 minutes. The fluidic layer was then cured for eight minutes at 80 °C. In the thin chip preparation, the fluidic layer (6:1, PDMS base to crosslinker ratio) was spun at 100 RPM (Laurell Technologies, Corp.), degassed under vacuum conditions for five minutes, and cured for four minutes at 80 ºC. Concurrently, an adapter piece with the corresponding access holes for the inlet and outlet ports on the device is casted using 50 grams of 10:1 PDMS base to crosslinker ratio, degassed for 30 minutes, and cured for eight minutes at 80 ºC. In both types of devices, the valve layer (15:1, PDMS base to crosslinker ratio) was spun at 1350 RPM (Laurell Technologies, Corp.) and cured for four minutes at 80 °C. After baking, the respective fluidic layer was manually aligned to the valve layer under a stereoscope. Both layers were then baked for 60 minutes at 80 °C for the thick chip and eight minutes at 80 ºC for the thin chip. Due to the substantial decrease in thickness of the thin chip, the baking times are significantly reduced and thus, decreasing the fabrication process time. Access holes were then punched for the inlet and outlet ports and the PDMS device was bonded to Thickness #1 cover glass (Ted Pella, Inc.) with oxygen plasma treatment. An additional

cover glass is bonded on top of the heating region of the device with oxygen plasma treatment. Concurrently, the adapter piece is aligned and bonded on top of the thin chip device. The device is kept under vacuum prior to use and operation. The thin chip fabrication technique helped address issues in droplet evaporation during device operation at high temperatures required for PCR and increased fabrication efficiency, and thus was the adopted technique. This fabrication schematic of the thin-chip is shown in **Figure 2.2.**

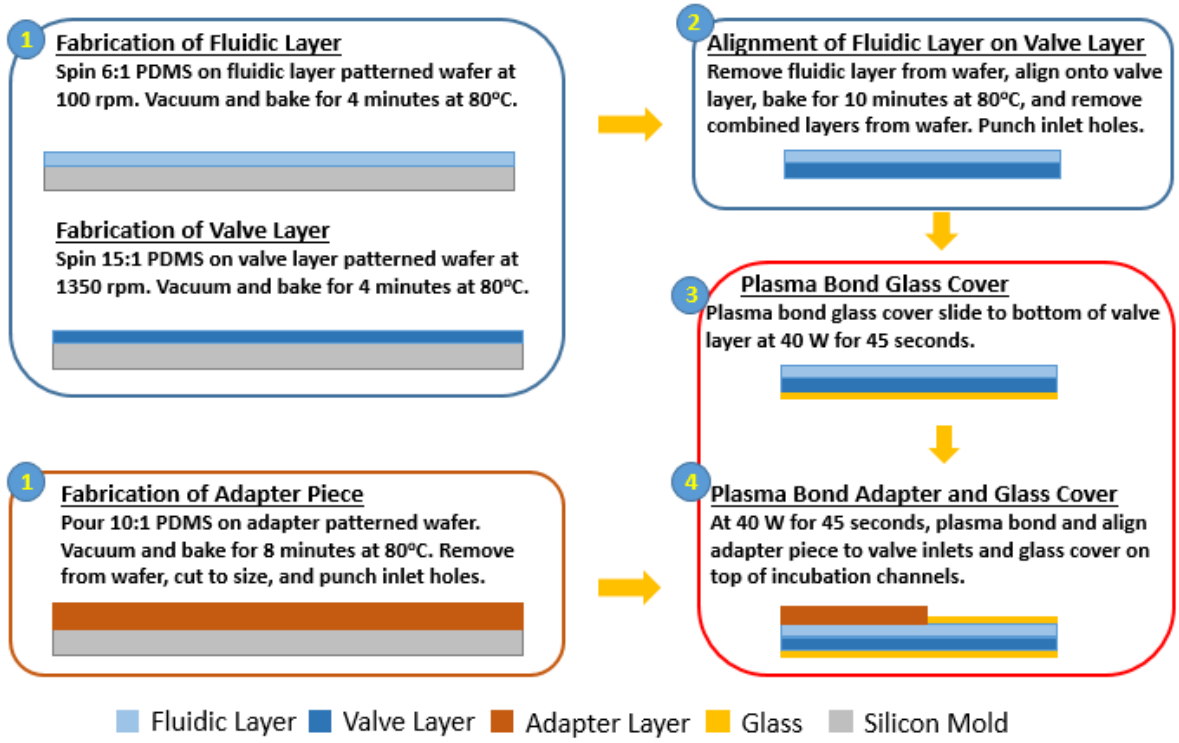

Figure 2.2: Thin-chip fabrication schematic. Fluidic layer, valve layer, and adapter layer are fabricated separately via soft lithography using patterned silicon wafers as templates. All layers are bonded together via heat and plasma treatment.

2.2.4 Device Operation

Each valve port on the device is individually connected to a solenoid valve via Tygon® tubing and needle tips. The solenoid valve system is regulated by a pressure controller, drawing house air to pressurize each valve on the device. The opening and closing of each solenoid

valve is operated by a custom MATLAB script. When the solenoid valve is ON, air flows and pressurizes the respective valve on the device, and collapses the corresponding fluidic channel above to CLOSE. Conversely, when the solenoid valve is OFF, air does not flow and the respective valve on the device is unpressurized, allowing the corresponding fluidic channel above to remain OPEN. The MATLAB script allows for customized opening and closing sequences and times of all the valves on the device, allowing for automation of device operation. Valves are operated at 20 PSI.

All valves are initially kept pressurized and closed. Millipore water is loaded through the carrier oil inlet and allowed to flow through the entire device. Carrier fluid is then interchanged and loaded through the carrier oil inlet and allowed to flow through the entire device. Because PDMS is a porous material, this serves to prime the device and saturate the PDMS pores to help prevent droplet evaporation and diffusion. Sample and reagents are then loaded in their respective inlets. Concurrently, Taqman PCR is performed on benchtop to confirm amplification results. Both carrier oil and samples are pressurized at 30 PSI. Droplet generation is controlled with the custom MATLAB script using a specific sequence that corresponds to each valve and each valve's opening and closing times, digitalizing the sample into nanoliter droplets. The carrier oil is flown through between each droplet to separate each sample droplet. The device is then mounted on the Peltier heating setup, in which two heating zones are used, 92 ºC and 60 ºC for thermocycling. FAM/VIC fluorescence detection and read out is simultaneously performed at the detection region using the optical set up.

2.2.5 Optimization of Carrier Fluid, Additives, and Surfactants

Optimization of the carrier fluid, sample additives, and surfactants was performed for the droplet-based Taqman PCR assay to overcome issues with droplet stability and small

reagent/fluorophore molecule diffusion out of the droplet. This poses challenges in which fluorescence readings of baseline were significantly elevated leading to poor amplification measurements and/or inconclusive results.

Different mixtures of fluorinated oils, including: FC-40, 1H, 1H, 2H, 2H-Perfluoro-1-octanol (Sigma Aldrich) (4:1 v/v) (PFO), and various viscosities of silicon oil (0 cSt, 5 cSt, 10 cSt, 50 cSt, 100 cSt, 200 cSt, and 350 cSt) were evaluated. The addition of bovine serum albumin (BSA) and Tween 20 of various concentrations in the sample preparation was evaluated for small hydrophobic molecule and fluorophore retention within droplets. The addition of BSA and Tween 20 increased fluorophore retention within the droplet, but also caused droplet sticking in the channels and poor droplet mobility. These results were consistent with those found in the literature (11). A mixture of BSA and Tween 20 and the use of high viscosity silicone oil (350 cSt) offered the optimal balance between droplet stability and small molecule retention among the carrier oils and surfactants that were evaluated.

2.2.6 Interface with Heating System

To achieve thermocycling, the microfluidic device was mounted on top of a Peltier heating setup coupled with a PID controller. The heating system consisted of three Peltier plates, in which each can be individually controlled by a corresponding PID controller. Although the Taqman PCR assay only required two temperatures for thermocycling, three Peltier plates were incorporated in the heating system design for flexibility in future assay-based devices and applications. The device is mounted such that the heating region of the device comes into direct contact with the corresponding Peltier plate, and the detection region is accessible to the excitation laser of the optical setup while the microfluidic device

simultaneously undergoes thermocycling with the heating system. The development of the heating system is described in the Results/Discussion section.

2.2.7 Fluorescence Detection and Data Analysis

Spectroscopy data was acquired using the same custom-built two-color confocal fluorescence spectroscope (CFS) as described for the Invader device **(Figure 1.4)**. It is designed to simultaneously detect both FAM and VIC fluorophores within droplets, using a dual laser excitation (488 nm, 552 nm) and dual emission channel (506-534 nm and 608-648 nm), with two silicon avalanche photodiodes (APD) for fluorescence detection, captured using a neutral density filter 2 (ND2). The spectroscopy platform also includes a trans-illumination LED and CCD camera for bright-field imaging (13). Fluorescence data is collected using a custom LabVIEW program GUI, in which traces of fluorescence data, in terms of photon count, is collected in 10 ms bins for 10 minutes. Fluorescence data is collected for droplets prior to entering the heating region for thermocycling and after exiting the heating region. In post processing and analysis of raw fluorescence data, all fluorescence traces files are concatenated together through MATLAB. A threshold is defined, separating droplet fluorescence from baseline carrier oil fluorescence, and the average photon count of each droplet is computed. The fluorescence of droplets before and after thermocycling of both DNA-containing droplets and negative control droplets are compared to determine allele callout and quantify DNA amplification. The fluorescence of the DNA-containing droplets is normalized by the fluorescence of the negative control droplets to determine degree of amplification.

2.3 Results and Discussion

2.3.1 Optimization of Carrier Fluid, Additives, and Surfactants

Following the successful development and performance of the Invader assay device, the same operation protocol was tested for the new, modified PCR device to perform the Taqman PCR assay. Rather than an isothermal incubation at 63 ^{o}C that was used for the Invader assay, the Taqman PCR assay necessitates thermocycling between 60 ^{o}C and a much higher, elevated temperature of 92 ^{o}C. Initial performance of the Taqman PCR assay on device was inconclusive – the fluorescence of the droplets was indistinguishable from the fluorescence of the baseline carrier oil. Furthermore, the fluorescence of the baseline carrier oil (FC40/PFO) was significantly elevated after thermocycling at high temperatures in comparison to the fluorescence of the baseline carrier oil before thermocycling. The elevated temperature of 92 ^{o}C facilitated fluorophores and small molecules diffusion out of the droplets and into the surrounding carrier oil, leading to lower droplet fluorescence intensities and higher baseline fluorescence intensities.

To address this issue, a variety of different carrier oils (silicone oil of varying viscosities) and droplet additives (different concentrations of BSA and Tween 20) were evaluated for fluorophore retention within the droplets. For a 10 uL sample preparation: 5 uL of KlearKall Buffer, 2 uL of DNA target, and 3 uL of H_2O was used. Varying concentrations of BSA and Tween 20 from 0% to 10% by volume combinations was added to the sample mixture in substitute of the water component to maintain the 10 uL sample preparation and evaluated. Initial benchtop testing on a standard PCR machine was done to confirm DNA amplification. As BSA concentration increased, PCR efficiency slightly increased. Concurrently, DNA sample droplets with BSA/Tween additives of corresponding concentrations were generated on the device to evaluate for droplet stability and mobility. Although the addition of BSA was

seen to increase amplification efficiency on benchtop, the addition of BSA increased droplet interaction with the PDMS channel walls, leading to droplets "sticking" and shearing within the device. Tween 20 acted as an appropriate surfactant surrounding the droplets, allowing it to maintain stable droplet movement and integrity. In compromise, 5% Tween 20 was added and 5% BSA was selected for the 10 uL sample preparation. A final preparation of 5 uL of KlearKall Buffer, 2 uL of DNA target, 0.5 uL of BSA, 0.5 uL of Tween 20, and 2 uL of H_2O was now adopted.

Next, silicone oil was evaluated as an alternative carrier oil to FC40/PFO. In separate modules, the PCR sample preparation detailed above was suspended in equal volumes of FC40/PFO, silicone oil (of varying viscosities), and no oil (control). These samples were amplified on benchtop, in which the fluorescence intensities of FAM (green) and VIC (red) were monitored on the PCR machine **(Figure 2.3)**.

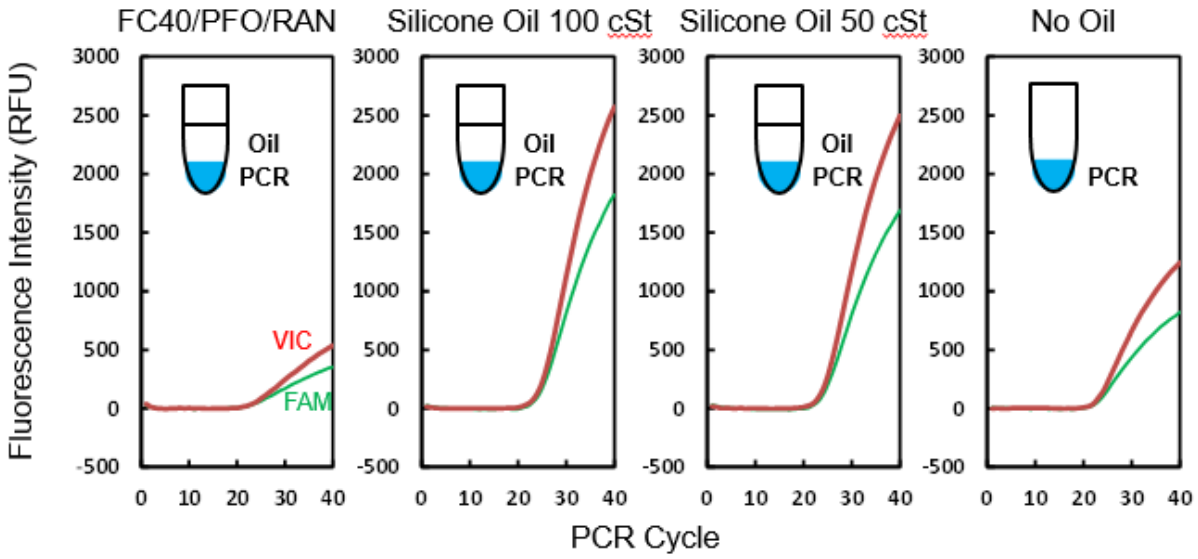

Figure 2.3: Fluorescence intensity over time of PCR sample mixed in various carrier oils: FC40/PFO, silicone oil, and no oil (control). Silicone oil is found to not inhibit PCR amplification. Fluorescence intensity of PCR sample in silicone oil is greater than the fluorescence intensity of the PCR sample in FC40/PFO and control, as well as exhibiting similar or slightly earlier onset of amplification.

It is seen that the presence of silicone oil does not inhibit the PCR reaction. Rather, the PCR sample suspended in silicone oil exhibited greater fluorescence intensities and similar, if not earlier amplification onset cycle than the PCR sample suspended in FC40/PFO and the control PCR sample without any additional carrier oil added. Following, the PCR products were collected and gel electrophoresis was performed to confirm amplification **(Figure 2.4A)**. The oil was also collected and fluorescence was measured to determine whether fluorophores diffused from the PCR sample into the surrounding oil **(Figure 2.4B)**.

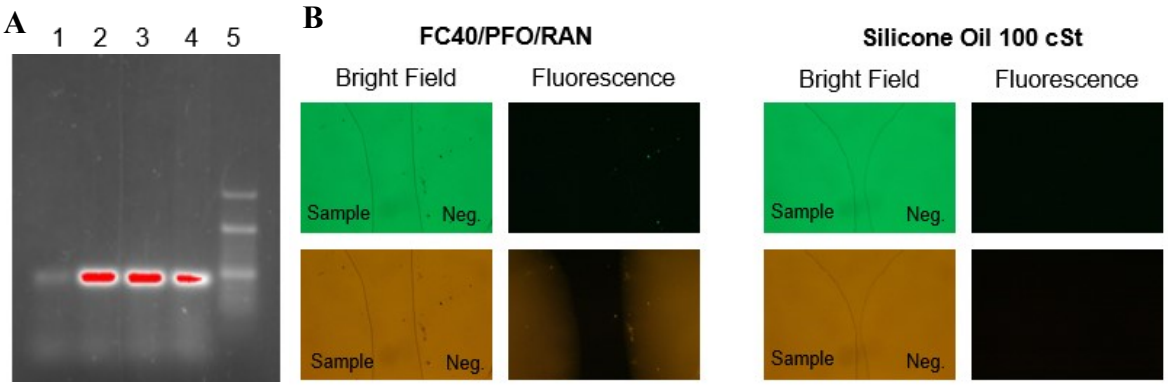

Figure 2.4: A) Gel electrophoresis of amplified PCR samples. Lane 1 to 5 is PCR products in FC40/PFO, silicone oil (100 cSt), silicone oil (50 cSt), no oil (control), and ladder. PCR amplification is greater in the presence of silicone oil than it is in FC40/PFO and exhibits similar if not greater amplification than that of the control. **B)** The oil is collected and fluorescence is measured. Fluorescence intensity is greater in FC40/PFO carrier oil, whereas no fluorescence is detected from the silicone oil.

As seen in the results of the gel electrophoresis of the PCR products, PCR amplification is confirmed to be greater in the presence of silicone oil than it is in FC40/PFO, and exhibits similar if not greater amplification that that of the control (no oil) as well. As seen in the fluorescence imaging of the carrier oils, the fluorescence intensity is present/greater in FC40/PFO, whereas no fluorescence is detected in the silicone oil. This indicates that minimal

amounts of fluorophores diffused out from the PCR sample into the surrounding carrier oil when silicone oil is used in comparison to the FC40/PFO carrier oil.

Next, the selected silicone oil is evaluated on the device. Benchtop amplified PCR sample mixture was prepared, loaded onto the device, and droplets were generated and observed for droplet stability using a corresponding carrier oil. In four separate experiments, the FAM fluorescence of the carrier oil – FC40/PFO or silicone oil – was measured in the detection region in the presence and absence of amplified PCR products in the device **(Figure 2.5)**.

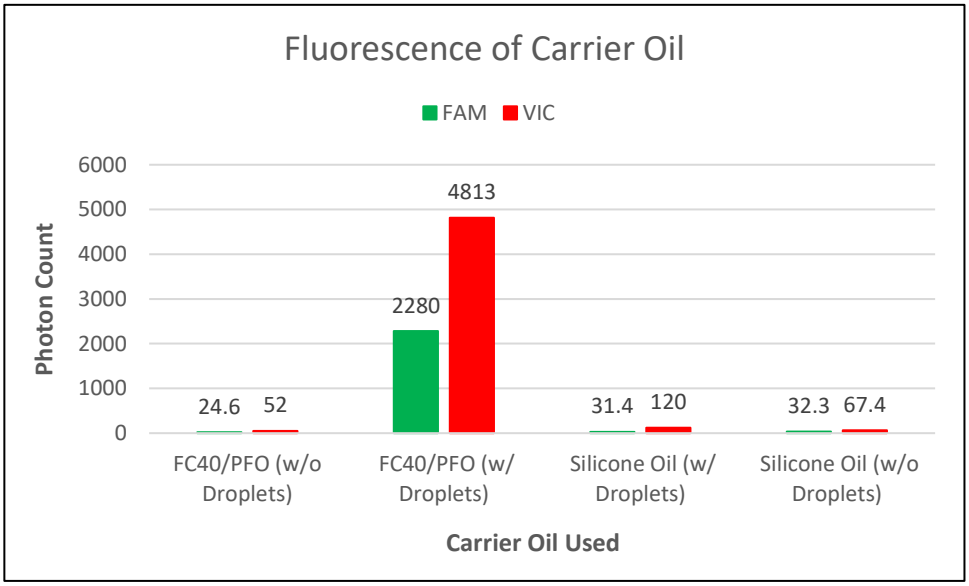

Figure 2.5: FAM and VIC fluorescence of baseline carrier oil – FC40/PFO or silicone oil – in the presence or absence of amplified PCR product droplets. Upon introduction of amplified PCR droplets, fluorescence of FC40/PFO spikes, whereas fluorescence of silicone oil remains the steady. Fluorescence is measured in the detection. For each carrier oil, FAM/VIC fluorescence of carrier oil without droplets is measured first. After measurement, amplified PCR product is loaded and droplets are generated and flown through the device. FAM/VIC fluorescence of baseline carrier oil is measured again. New device is used for each carrier oil evaluated.

As seen, the fluorescence of the baseline silicone oil in the absence of amplified PCR droplets was 32.3 **(Figure 2.5, Silicone Oil without Droplets)**. In the presence of amplified PCR products droplets, the fluorescence of the baseline silicone oil maintained steady, measuring at 31.4 **(Figure 2.5, Silicone Oil with Droplets)**. Similarly, the fluorescence of the baseline FC40/PFO carrier oil in the absence of amplified PCR product droplets was also low, at 24.6 **(Figure 2.5, FC40/PFO without Droplets)**. However, when amplified PCR products were introduced into the device, the baseline fluorescence of the FC40/PFO carrier oil spiked to 2280.0 **(Figure 2.5, FC40/PFO with Droplets)**. This supports that fluorophores rapidly diffuse out of PCR sample droplets and into surrounding FC40/PFO oil, whereas silicone oil does a good job of fluorophore/small molecule retention within the droplets. Similar results were found in the VIC channel fluorescence measurements.

Concurrently, FAM/VIC fluorescence is measured of the amplified PCR product droplets. The FAM/VIC fluorescence of the amplified PCR product droplets is normalized with respective to its negative control sample droplets (contains no DNA products) **(Figure 2.6)**.

As seen, normalized fluorescence values of the amplified PCR droplets in silicone oil (5.2 and 11.7) are greater in both FAM and VIC fluorescence measurements, respectively than in FC40/PFO as a carrier oil (3.6 and 1.4). Thus, in comparison to FC40/PFO, using silicone oil as an alternative carrier oil, we see higher droplet fluorescence intensities and lower baseline fluorescence intensities, suggesting greater fluorophore retention within the droplets and increased abilities to accurately distinguish and quantify successful amplification.

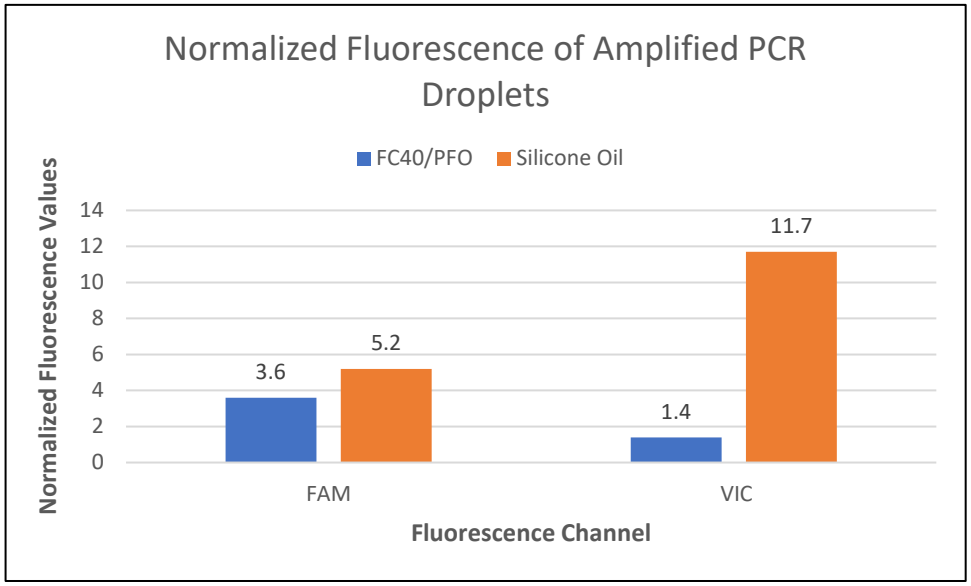

Figure 2.6: FAM/VIC fluorescence of amplified PCR product droplets normalized with respect to the corresponding negative control droplets (without DNA) in FC40/PFO and silicone oil. Fluorescence is measured at the detection region and conducted concurrently to fluorescence data gather in **Figure 2.5**. Silicone oil exhibits greater fluorophore retention within droplets and more distinguishable measures of amplification.

2.3.2 Redesign of Heating System

As mentioned, the Taqman-based PCR assay requires thermocycling between two temperatures – a high, elevated temperature of 92 ºC and a lower temperature of 60 ºC. In order to successfully amplify the target DNA, the temperatures must be precise and accurate to allow for proper activation of the hot-start enzyme, successful denaturation of the double stranded DNA, and elongation of the amplified DNA products. Because of the importance of precise temperature control, the previously built Peltier heating system was re-evaluated. In the design of the old Peltier heating system **(Figure 2.7)**, the heating system consists of a solid aluminum plate. In the heating region, there are three temperature zones and plates. Each temperature zone is heated by a Peltier plate that is thermally glued directly underneath each temperature

zone. Each Peltier plate can be individually controlled by a PID controller to set at a specific temperature. Directly underneath the Peltier plates is a small fan and heat sink to help regulate and stabilize the temperature. The device is placed on the aluminum plate and is indirectly heated by the Peltier plate system underneath.

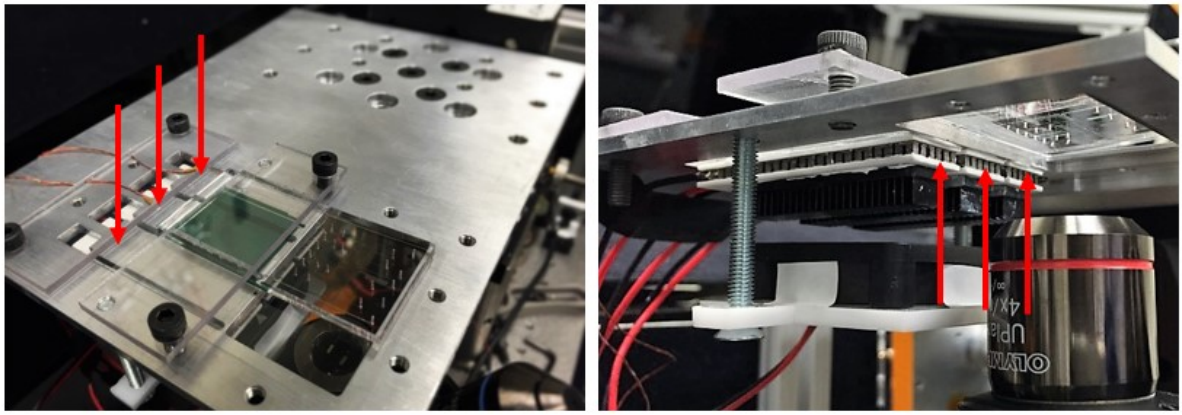

Figure 2.7: Photograph of old heating system, consisting of a solid aluminum plate interface. The three arrows (left) indicate the three temperature zones that the microfluidic device is placed on. Directly underneath each temperature zone are three individual Peltier plates, indicated by the three arrows (right). Each Peltier plate can be individually set at a specific temperature via PID controllers, directly heating the aluminum plate and indirectly heating the microfluidic device above. Attached beneath the three Peltier plates is a heat sink and a fan to regulate and stabilize the temperatures.

To evaluate the temperature accuracy and precision of the heating system, the two respective Peltier plates were set at Taqman PCR assay temperatures, 92 ºC and 60 ºC. An external thermocouple is used to measure the actual temperature on the aluminum heating plate. On each temperature plate, three spots (top, middle, and bottom) are selected and the temperature is measured at each location to determine its accuracy and spatial variation across a plate set a constant temperature **(Figure 2.8)**.

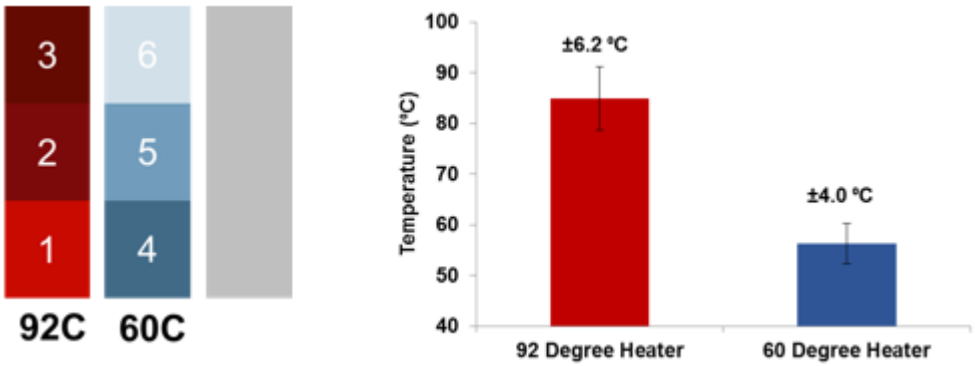

Figure 2.8: (Left) The three locations on each the 92 ºC temperature plate and the 60 ºC temperature are indicated. An external thermocouple is used to measure the temperature at these locations. (Right) The results indicated a spatial variation of +/- 6.2 ºC across the plate set at 92 ºC and a spatial variation of +/- 4 ºC across the plate set at 60 ºC, both with a lower temperature average than the value set.

The results indicate a large spatial variation of +/- 6.2 ºC across the temperature plate set at 92 ºC and a similar large spatial variation of +/- 4 ºC across the temperature plate set at 60 ºC, both with a temperature average lower than the temperature set for the respective plate. This inaccuracy and imprecision of temperature control is largely due to an indirect contact from the actual Peltier plate heating source that serves to heat the aluminum plate. Heat can be loss during this heating process; there is no direct contact. In addition, the Peltier plates are thermally glued to the aluminum plate. A non-uniform application of the thermal glue may also lead to temperature variations across the aluminum plate. Lastly, aluminum as a material is conductive and may draw heat further away from the temperature zones that is intended to heat the microfluidic device.

A new heating plate is designed to address these issues **(Figure 2.9)**. In the new heating system design, the aluminum plate is removed. It is replaced using PVC material as the stage. PVC, a synthetic plastic polymer, acts as a good thermal insulator, minimizing heat loss through the plate itself. In addition, the three temperature zone plates are removed and replaced

by a pocket in the plate. The pocket is sized such that the three Peltier plates fits snuggly within the pocket, flush with the surface of the PVC heating plate. In this design, the microfluidic device will be placed directly on top of the Peltier plates and comes into direct contact with the heating source. Thus, the indirect heating and the non-uniform application of thermal glue is bypassed. Beneath the Peltier plates is a fan and heat sink to regulate and stabilize the temperatures.

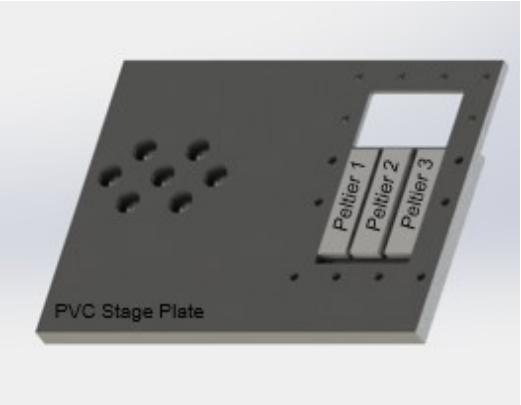

Figure 2.9: CAD-designed, new heating system consisting of a PVC heating platform with a pocket sized to snuggly fit three Peltier plates flush with the surface of the PVC heating stage.

To evaluate the improved heating system, the same evaluation was done in which an external thermocouple was used to measure the temperatures across each Peltier plate set at their respective temperatures of 92 ºC and 60 ºC **(Figure 2.10)**. A commercially available flatbed thermocycler is also measured as a control comparison.

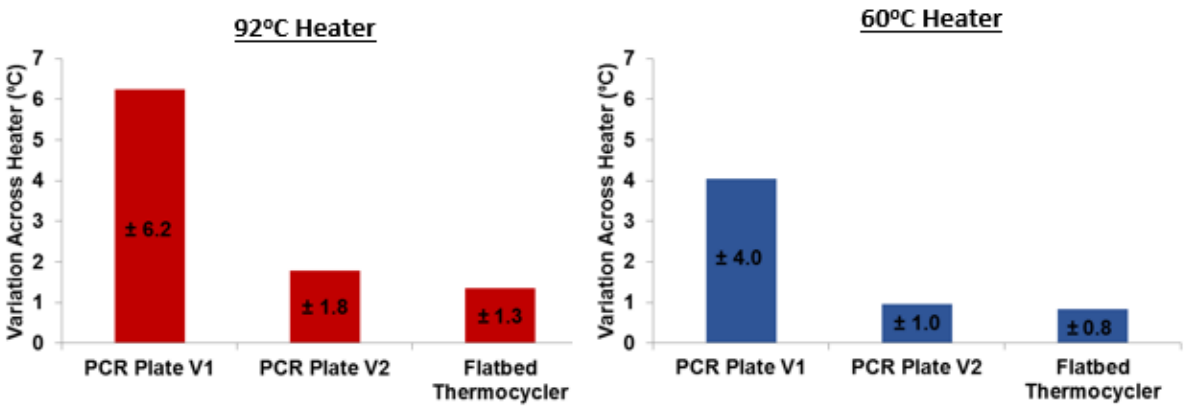

Figure 2.10: Temperature is measured across each Peltier plate in the same locations as indicated before (Figure 3.8) set at 92 ºC and 60 ºC, respectively. "PCR Plate V1" is the old heating system, "PCR Plate V2" is the newly designed heating system, and "Flatbed Thermocycler" is a commercially available machine/heating plate used heating, used a control comparison.

The results indicate a significantly lower spatial variation across each Peltier plate. In comparison, the spatial variation across the Peltier plate set at 92 ºC decreased from +/- 6.2 ºC to +/- 1.8 ºC in the newly designed heating plate. This spatial variation is very similar to the spatial variation measured on a commercially available flatbed thermocycler, +/- 1.3 ºC. Similarly, the spatial variation the Peltier plate set at 60 ºC decreased from +/- 4.0 ºC to +/- 1.0 ºC, wherein the spatial variation measured on the commercially available flatbed thermocycle was +/- 0.8 ºC. The newly designed heating plate system provides increased temperature control, accuracy, and precision necessary for Taqman PCR assay.

2.3.3 On-Chip Amplification of DNA Samples

After optimization of the carrier oil, sample additives, and surfactants to address issues in fluorophore diffusion (Section 2.3.1), re-designing of the heating system address issues in temperature variation and control (Section 2.3.2), and adoption of a thin chip fabrication technique to address issues in evaporation (Section 2.2.3), these steps were collectively

implemented to perform PCR of un-amplified DNA samples within droplets on the device. The optimized PCR mixture was prepared on benchtop, using a DNA target homozygous in FAM fluorescence and loaded into the device via the sample inlets. The custom MATLAB was used to generate droplets in a repeated, specific sequence of one ROX dye droplet, one negative control (NTC) droplet, one ROX dye droplet, and two DNA-template containing droplets at one-minute intervals using silicone oil as the carrier oil that separates each droplet. ROX dye droplets display a strong VIC fluorescence and are used as spatial indicators of the sequence of droplets generated. Because the DNA target is homozygous in FAM fluorophore, a large fluorescence in the VIC channel and low fluorescence in the FAM channel will indicate a ROX droplet and allow us to identify the droplet sequence during analysis. The device is then secured onto the heating plate and FAM/VIC fluorescence is simultaneously detected and measured prior to and post thermocycling. An increase in FAM fluorescence for DNA-template containing droplets from before thermocycling to after thermocycling indicate DNA amplification. Whereas, we expect the fluorescence of NTC droplets to remain roughly the same before and after thermocycling, since no DNA templates are present.

Two heating systems/droplet dynamics are implemented: 1) A static heating system in which the sequence of droplets is repeatedly generated until the entirety of the heating region is filled with droplets. Once filled, the flow of the carrier oil was stopped and the motion of the droplets was halted. The device is then secured onto the heating plate, such that the heating region is on both Peltier plates. Both Peltier plates are now simultaneously set at 92 ^{o}C for 3 minutes, and then cycled at 92 ^{o}C for 45 seconds and 60 ^{o}C for 45 seconds, for 30 cycles. In this system, the droplets do not move, and are thus static, while the temperature of Peltier plates itself cycles. This system was initially implemented to best mimic the conditions of a traditional

PCR machine that uses a static, flatbed thermocycler. Fluorescence is measured before and after thermocycling. A representative fluorescence trace is shown in **Figure 2.11**.

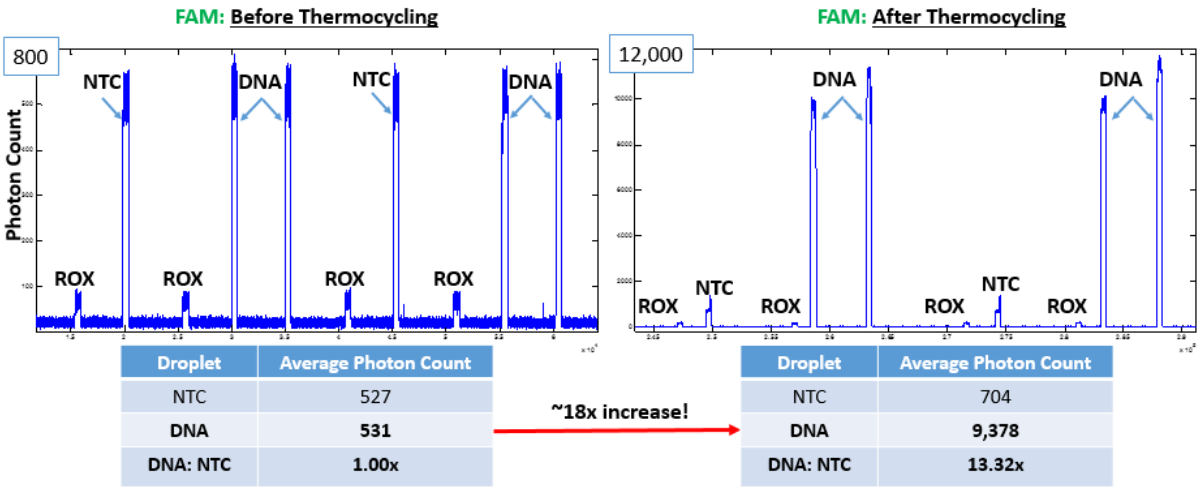

Droplet	Average Photon Count
NTC	527
DNA	531
DNA: NTC	1.00x

Droplet	Average Photon Count
NTC	704
DNA	9,378
DNA: NTC	13.32x

Figure 2.11: Representative FAM fluorescence traces before and after thermocycling in a static heating system. The average fluorescence of DNA-containing droplets demonstrates a 17.66-fold increase from before thermocycling (531) to after thermocycling (9,378). The fluorescence ratio between DNA-containing droplets and NTC droplets is 13.32, where the fluorescence of NTC droplets remain approximately the same.

As seen, the average fluorescence of DNA-containing droplets demonstrates a 17.66-fold increase from a fluorescence of 531 before thermocycling to a photon count of 9,378 after thermocycling. Whereas, the average fluorescence of NTC droplets remain approximately the same, with an average photon count of 527 before thermocycling and 704 after thermocycling. The fluorescence ratio between DNA-containing droplets and NTC droplets before thermocycling is 1.00 while the fluorescence ratio after thermocycling is 13.32, indicating DNA amplification did occur.

Next a dynamic, continuous-flow heating system was implemented. In this setup, the sequence of droplets is continuously generated and the device is secured to the heating plate

such that the hot start channel and half of the heating region sits on top of the 92 ºC Peltier plate and other half of the heating region sits on top of the 60 ºC Peltier plate. The Peltier plate temperatures remain fixed, while the droplets continuously move between each temperature zone – three minutes in the 92 ºC hot-start region, followed by 45 seconds in the 92 ºC temperature zone and then 45 seconds in the 60 ºC temperature zone, as the droplets cycle back and forth between the two temperature zones in the serpentine, heating region. The precise timing is dictated by the speed of the droplets which is adjusted by the back pressure of the carrier oil. FAM/VIC fluorescence is continuously measured and a representative fluorescence trace is shown in **Figure 2.12**.

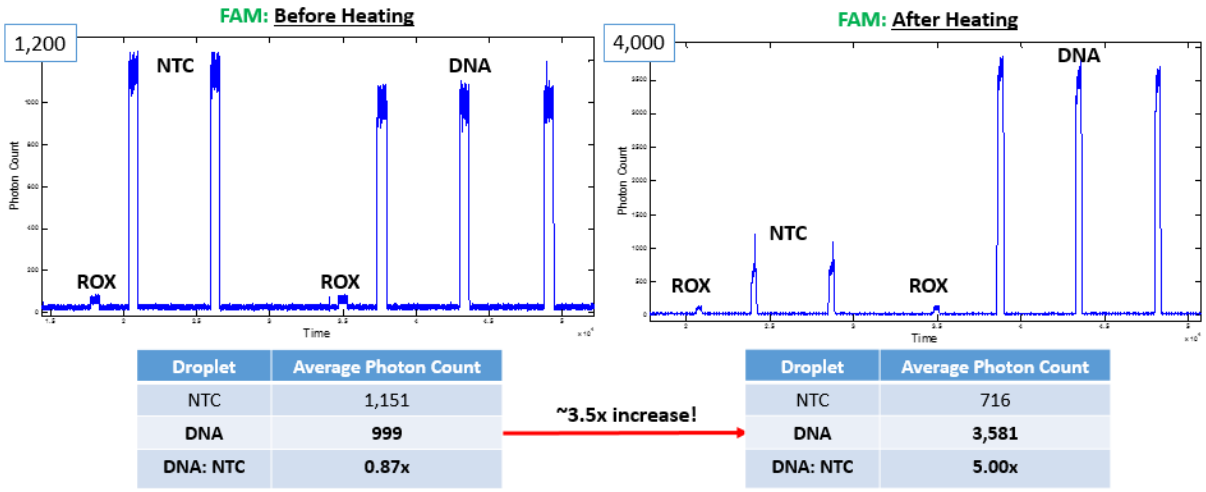

Droplet	Average Photon Count
NTC	1,151
DNA	999
DNA: NTC	0.87x

Droplet	Average Photon Count
NTC	716
DNA	3,581
DNA: NTC	5.00x

Figure 2.12: Representative FAM fluorescence traces before and after thermocycling in a **dynamic, continuous-flow** heating system. The average fluorescence of DNA-containing droplets demonstrates a 3.5-fold increase from before thermocycling (999) to after thermocycling (3,581). The fluorescence ratio between DNA-containing droplets and NTC droplets is 5.00, where the fluorescence of NTC droplets remain approximately the same.

As seen, the average fluorescence of DNA-containing droplets demonstrates a 3.5-fold increase from a fluorescence of 999 before thermocycling to a photon count of 3,581 after thermocycling. Whereas, the average fluorescence of NTC droplets remain approximately the

same, with an average photon count of 1,151 before thermocycling and 716 after thermocycling. The fluorescence ratio between DNA-containing droplets and NTC droplets before thermocycling is 0.87 while the fluorescence ratio after thermocycling is 5.00, indicating DNA amplification did occur.

2.4 Conclusion

This chapter detailed the initial development of an integrated microfluidic platform for on-chip, continuous flow PCR for DNA amplification and genotyping. Several challenges were met – optimization of the carrier oil, sample additives, and surfactants to address issues in fluorophore diffusion, re-designing of the heating system address issues in temperature variation and control, and adoption of a thin chip fabrication technique to address issues in evaporation to demonstrate significant amplification results in the static PCR system and promising DNA amplifications results in the dynamic PCR system.

There are several, immediate future directions with the PCR device to push the technology forward. As seen in the initial results, there is a large difference in the magnitude of amplification between the static PCR system and dynamic PCR system. Although promising, the dynamic PCR system can be further optimized to exhibit similar degree of DNA amplification as seen by the static PCR system. In addition, a library of DNA targets and probes can be multiplexed on-chip similar to what was done on the Invader microfluidic platform to demonstrate the enhanced capabilities of the platform and accuracy with multiple samples.

By integrating PCR onto the chip, this microfluidic device eliminates prior benchtop assay preparation. Similar to the promises of the Invader device, sample loading can be interfaced and automated with sample loading robotics. Once coupled with the sample loading

system, this microfluidic device will truly become a stand-alone, continuous-flow device for high-throughput PCR and genotyping.

REFERENCES

1. National Academies of Sciences, Engineering, and Medicine. *Genetically Engineered Crops: Experiences and Prospects*. National Academies Press, 2017.

2. Thomson, M.J. (2014) High-throughput SNP genotyping to accelerate crop improvement. *Plant Breeding and Biotechnology*, 2, 195-212.

3. Fan, J.B., Oliphant, A., Shen, R., Kermani, B.G., Garcia, F., Gunderson, K.L., Hansen, M. Steemers, F., Butler, S.L., Deloukas, P. *et al.* (2003) Highly parallel SNP genotyping. *Cold Spring Harbor symposia on quantitative biology*, 68, 69-78.

4. Hyten, D.L., Song, Q., Choi, I.Y., Yoon, M.S., Specht, J.E., Matukumalli, L.K., Nelson, R.L., Shoemaker, R.C., Young, N.D. and Cregan, P.B. (2008) High-throughput genotyping with the GoldenGate assay in the complex genome of soybean. *TAG. Theoretical and applied genetics. Theoretische und angewandte Genetik*, 116, 945-952.

5. Shen, R., Fan, J.B., Campbell, D., Chang, W., Chen, J., Doucet, D., Yeakley, J., Bibikova, M., Wickham Garcia, E., McBride, C. *et al.* (2005) High-throughput SNP genotyping on universal bead arrays. *Mutation research*, 573, 70-82.

6. Steemers, F.J., Chang, W., Lee, G., Barker, D.L., Shen, R. and Gunderson, K.L. (2006) Whole-genome genotyping with the single-base extension assay. *Nature methods*, 3, 31-33.

7. Hoffmann, T.J., Kvale, M.N., Hesselson, S.E., Zhan, Y., Aquino, C., Cao, Y., Cawley, S., Chung, E., Connell, S., Eshragh, J. *et al.* (2011) Next generation genome-wide association tool: design and coverage of a high-throughput European-optimized SNP array. *Genomics*, 98, 79-89.

8. Bardin, D., Kendall, M.R., Dayton, P.A. and Lee, A.P. (2013) Parallel generation of uniform fine droplets at hundreds of kilohertz in a flow-focusing module. *Biomicrofluidics*, 7, 34112.

9. Lyamichev, V., Mast, A.L., Hall, J.G., Prudent, J.R., Kaiser, M.W., Takova, T., Kwiatkowski, R.W., Sander, T.J., de Arruda, M., Arco, D.A. *et al.* (1999) Polymorphism identification and quantitative detection of genomic DNA by invasive cleavage of oligonucleotide probes. *Nature biotechnology*, 17, 292-296.

10. Lyamichev, V.I., Kaiser, M.W., Lyamicheva, N.E., Vologodskii, A.V., Hall, J.G., Ma, W.P., Allawi, H.T. and Neri, B.P. (2000) Experimental and theoretical analysis of the invasive signal amplification reaction. *Biochemistry*, 39, 9523-9532.

11. Courtois, F., Olguin, L.F., Whyte, G., Theberge, A.B., Huck, W.T., Hollfelder, F. and Abell, C. (2009) Controlling the retention of small molecules in emulsion microdroplets for use in cell-based assays. *Analytical chemistry*, 81, 3008-3016.

12. Rane, T.D., Zec, H.C. and Wang, T.H. (2015) A barcode-free combinatorial screening platform for matrix metalloproteinase screening. *Analytical chemistry*, 87, 1950-1956.

13. Rane, T.D., Chen, L., Zec, H.C. and Wang, T.H. (2015) Microfluidic continuous flow digital loop-mediated isothermal amplification (LAMP). *Lab on a chip*, 15, 776-782.

14. Rane, T.D., Puleo, C.M., Liu, K.J., Zhang, Y., Lee, A.P. and Wang, T.H. (2010) Counting single molecules in sub-nanolitre droplets. *Lab on a chip*, 10, 161-164.

15. Rane, T.D., Zec, H.C. and Wang, T.H. (2012) A serial sample loading system: interfacing multiwell plates with microfluidic devices. *Journal of laboratory automation*, 17, 370-377.

16. Koster, S., Angile, F.E., Duan, H., Agresti, J.J., Wintner, A., Schmitz, C., Rowat, A.C., Merten, C.A., Pisignano, D., Griffiths, A.D. *et al.* (2008) Drop-based microfluidic devices for encapsulation of single cells. *Lab on a chip*, 8, 1110-1115.

17. Baret, J.C., Miller, O.J., Taly, V., Ryckelynck, M., El-Harrak, A., Frenz, L., Rick, C., Samuels, M.L., Hutchison, J.B., Agresti, J.J. *et al.* (2009) Fluorescence-activated droplet sorting (FADS): efficient microfluidic cell sorting based on enzymatic activity. *Lab on a chip*, 9, 1850-1858.

CURRICULUM VITAE

Tony J. Zheng
3121 Chase Drive, Fort Collins, Colorado 80525
Telephone: 970-817-4981; Email: tonyjzheng@gmail.com

EDUCATION

2017 – Present **Doctorate of Medicine and Philosophy (MD-PhD)**
Oregon Health & Science University, Portland OR

2015 – 2017 **Masters of Science and Engineering in Biomedical Engineering**
Johns Hopkins University, Baltimore MD
GPA: 3.70

2011 – 2015 **Bachelors of Science in Biomedical Engineering (BS)**
Johns Hopkins University, Baltimore MD
GPA: 3.66

RESEARCH AND WORK EXPERIENCE

Masters/Graduate Researcher
July 2015 – Present
BioMEMS & Single Molecule Dynamics Lab, Johns Hopkins University, Baltimore, MD
Dr. Jeff Tza-Huei Wang, Ph.D., Professor of Biomedical Engineering

- Development of continuous-flow, droplet-based, microfluidic PCR device for high-throughput genotyping
- Development of low-cost, embedded solder electrodes for impedance-based feedback control in microfluidic devices
- Data collection and finalization of digital microfluidic device for single DNA molecule PCR amplification

Summer Intern Researcher
May 2014 – August 2014
The Sound Sleep Project, Sleep Lab, Johns Hopkins University, Baltimore, MD

- Part-time intern researcher – 25 hours/week
- Research: Understanding of how sleep interacts with cognition in healthy people across the life cycle, in brain diseases, and in sleep disorders; created programs using MATLAB to analyze the absence of stimulation and its effect on sleep

Undergraduate Researcher
January – August 2013
Neurology Science/Stroke Lab, Johns Hopkins Bayview Medical Center, Baltimore, MD
Dr. Steven Zeiler, M.D., Ph.D., Assistant Professor of Neurology

- Research was focused on behavioral, molecular, and anatomical studies of translational mouse models of stroke and post-stroke plasticity; conducted behavioral training of mice, prepared brain tissue samples, and data collection